

¹ Bayesian inference of prehistoric population dynamics from multiple
² proxies: a case study from the North of the Swiss Alps

³ Martin Hinz^{1,2,*} Joe Roe¹ Julian Laabs³ Caroline Heitz³ Jan Kolář^{4,5}

⁴ 30 Mai, 2022

⁵ **Abstract**

Robust estimates of population are essential to the study of human–environment relations and socio-ecological dynamics in the past. Population size and density can directly inform reconstructions of prehistoric group size, social organisation, economic constraints, exchange, and political and social institutions. In this pilot study, we present an approach that we believe can be usefully transferred to other regions, as well as refined and extended to greatly advance our understanding of prehistoric demography. Here, we present a Bayesian hierarchical model that uses Poisson regression and state-space representation to produce absolute estimates of past population size and density. Using the area North of the main ridge of the Swiss Alps in prehistoric times (−1000 BCE) as a case study, we show that combining multiple proxies (site counts, radiocarbon dates, dendrochronological dates, and landscape openness) produces a more robust reconstruction of population dynamics than any single proxy alone. The model’s estimates of the credibility of its prediction, and the relative weight it affords to individual proxies through time, give further insights into the relative reliability of the evidence currently available for paleodemographic research. Our prediction of population development of the case study area accords well with the current understanding in the wider literature, but provides a more precise and higher-resolution estimate that is less sensitive to spurious fluctuations in the proxy data than existing approaches, especially the popular summed probability distribution of radiocarbon dates. The archaeological record provides several potential proxies of human population dynamics, but individually they are inaccurate, biased, and sparse in their spatial and temporal coverage. Similarly, current methods for estimating past population dynamics are often simplistic: they work on limited spatial scales, tend to rely on a single proxy, and are rarely able to infer population size or density in absolute terms. In contemporary demography, it is becoming increasingly common to use Bayesian statistics to estimate population trends and project them into the future. The Bayesian approach is popular because it offers the possibility of combining heterogeneous data, and at the same time quantifying the uncertainty and credibility attached to forecasts. These same characteristics make it well-suited to applications to archaeological data in paleodemographic studies.

³⁰ ¹ Institute of Archaeological Sciences, University of Bern

³¹ ² Oeschger Centre for Climate Change Research, University of Bern

³² ³ CRC 1266 - Scales of Transformation, University of Kiel

³³ ⁴ Department of Vegetation Ecology, Institute of Botany of the Czech Academy of Sciences

³⁴ ⁵ Institute of Archaeology and Museology, Faculty of Arts, Masaryk University

³⁵ * Correspondence: Martin Hinz <martin.hinz@iaw.unibe.ch>

³⁶ Keywords: Prehistoric demography; Bayesian modelling; Multi-proxy; Settlement dynamics

³⁷ Highlights: - Bayesian modelling can integrate multiple, heterogeneous population proxies from the archaeological record - Our initial model produces more robust, high-resolution estimates of past population dynamics than previous, single-proxy approaches - We provide absolute estimates of population size and density on the area north of the Swiss Alps in prehistoric times (−1000 BCE)

41 **1. Introduction**

42 **1.1. Prehistoric demography**

43 Prehistorians have long recognised demography as a fundamental force in human cultural evolution (Childe,
44 1936). However, despite decades of interest in the demographic dynamics of prehistoric societies, concrete
45 estimates of population size and population density before written records remain elusive. Though the
46 archaeological record provides multiple possible demographic proxies (Hassan, 1981), lack of access to
47 this data, and a lack of methodological tools for turning it into quantitative estimates, has often left the
48 conclusions drawn from it vague and superficial (Hassan, 1981). As a result, ‘expert estimates’ transferred
49 from ethnographic parallels have often taken the place of direct inference from archaeological evidence Turchin
50 et al. (2015).

51 Early attempts to estimate the size and density of prehistoric populations from archaeological remains
52 were made by Hack (1942), Colton (1949), Frankfort (1950) and Cook (1946). Cook and Heizer Cook and
53 Heizer (1968) and Naroll (1962) provided rules derived from ethnographic contexts for estimating the size
54 of prehistoric populations. Cook and Heizer (1966) also made the first attempt to estimate the population
55 growth rate during the Neolithic (Hassan, 1981). These approaches became increasingly common after the
56 1960s, with the emergence of processual archaeology and its focus on human–environment relations and
57 population ecology (Hassan, 1981).

58 Following a spell out of fashion with the post-processual turn, prehistoric demography has experienced a revival
59 in recent years as part of the cultural evolution paradigm (Riede, 2009 and others in same issue; Shennan,
60 2000). Part of this resurgence can be explained by a renewed interest in human–environment relations and
61 human impact on the natural environment, which necessarily requires an assessment of population size.
62 Kintigh et al. (2014), for example, list human influence, dominance, population size, and population growth
63 amongst their ‘grand challenges’ for archaeology in the 21st century.

64 But methodological advances have certainly also played a role. In the last decade, the ‘dates as data’ technique
65 (Rick, 1987), which uses the frequency of radiocarbon dates as a proxy for population dynamics, was taken
66 up and significantly developed in a series of publications from the UCL group (e.g. Shennan et al., 2013),
67 and has since been widely applied to archaeological contexts around the world (Crema, 2022).

68 The ‘dates as data’ or summed radiocarbon approach has contributed greatly to our understanding of
69 prehistoric demography, but it is not without its critics Carleton and Groucutt (2021). While the methodology
70 continues to evolve and address these critiques (Crema, 2022), it remains subject to certain fundamental
71 problems common to all approaches that rely on a single proxy Schmidt et al. (2021). We believe that
72 these problems cannot be overcome by methodological refinements in this area alone. Instead, the Bayesian
73 approach we develop in this paper offers a robust, quantitative methodology for inferring prehistoric population
74 dynamics from multiple proxies, including summed radiocarbon dates.

75 **2. Background**

76 **2.1. Existing approaches to population estimation**

77 Müller and Diachenko (2019) have compiled a list proxies currently used for the estimation of population
78 size in prehistory. These can be roughly divided into three groups: ethnographic analogies; deductive
79 estimates from ecological/economic factors; and the interpolation of frequencies of archaeological features
80 (e.g. settlements, structures, individual finds). Three basic problems are common to all these approaches:

- 81 **1. Reliance on single proxy:** Most investigations are using only one source of evidence. Although
82 multi-proxy approaches exist, in such cases the individual proxies only serve to support each other
83 or the proxy used as the main estimator. There is no explicit combination of results to reduce the
84 inaccuracy and biases inherent to single proxies.
- 85 **2. Uncertainty in measurements:** All archaeological evidence comes with an inherent uncertainty
86 which is carried through to derived measurements. However, in most studies of prehistoric population,

87 individual curves are presented as estimates, and the potential error associated with these estimates is
88 almost never specified.

- 89 3. **Lack of a transfer function:** By ‘transfer function’, we mean something that allows for the proxy
90 data to be interpreted in terms of actual population size or density. This could be absolute, i.e. a
91 numerical estimate of population, or relative, i.e. a means of scaling changes in the proxy value to
92 changes in population. Lack of a suitable frameworks and ‘calibration’ data means that this is rarely
93 presented alongside proxy estimates. In the best case scenario, there will be a qualitative assessment
94 of the informative value of the proxy, but this does not sufficiently account for the complex nature of
95 archaeological data.

96 Furthermore, the types of archaeological data commonly used as population proxies share a number of
97 problematic characteristics. They are:

- 98 • **Limited:** We have only incomplete data that can be used for these purposes, and they are usually not
99 very informative.
100 • **Unevenly distributed:** For example, although there is a good data on settlement frequencies for
101 some regions, and these are sometimes have a very high temporal resolution, these regions are very
102 unevenly distributed over time and space.
103 • **Noisy:** Frequently individual proxies are strongly influenced by factors unrelated to population, for
104 example taphonomic conditions or depositional biases.
105 • **Unreliable:** Research strategies, research history and varying levels of resources available to researchers
106 strongly affect the nature of compiled datasets. As a result, systematic distortions are the rule rather
107 than the exception.
108 • **Heterogeneous:** A wide range of proxies can potentially inform us about population dynamics, all
109 with different spatio-temporal scales, granularity, information value, scales, and data formats.
110 • **Indirect:** We will never have direct data on prehistoric population; only proxy data that is thought
111 to be a reasonable substitute for it. The transfer functions that link the proxy data with the desired
112 quantity (population) are unknown. At best, they may be estimated by comparison with historical
113 examples or the (ethnographic) present. However, since living conditions, circumstances and economic
114 parameters differ greatly between the recent history and prehistory, these transfer functions can only
115 be considered a rough first approximation.
116 • **Contradictory:** When considering several proxies, differences in transfer functions, data quality and
117 noisiness inevitably lead to different results. The most common way to deal with this is to reject certain
118 proxies for a certain time periods, but this is not performed on a consistent or quantitative basis.

119 Here we argue that many, if not all, of these problems can be ameliorated through a) the explicit, quantitative
120 integration of multiple proxies; and b) the use of a Bayesian approach to take account of and estimate
121 uncertainty.

122 2.2. Hierarchical Bayesian demographic models

123 Many of the problems with archaeological population proxies are also encountered in contemporary demography.
124 In response, demographers have increasing turned to Bayesian methods to estimate and forecast contemporary
125 population dynamics. For example, Bryant and Zhang (2018) consider Bayesian data modelling a solution to
126 exactly the kind of problems that affect archaeological data. Specifically, Bayesian approaches are well suited
127 for limited, unreliable and noisy data. Various sources of data, even contradictory data, can be brought into
128 a common framework and used to support one another. These methods also provide a quantitative estimate
129 of the likelihood and uncertainty of the model’s resulting predictions (or in our case retro-dictions). Bayesian
130 approaches are also capable of accounting for spatially and temporally incomplete data: where this data is
131 missing, the uncertainty automatically increases, but this does not prevent general modelling and estimation.
132 Finally, hierarchically-structured model suites, in which sub-models are created for each individual proxy, can
133 be used to estimate transfer functions between individual proxies and the value to be modelled, thanks to the
134 interaction of a large number of data sources and evidence.

135 This modeling technique can thus be used to combine different lines of evidence horizontally and vertically
136 and in this way combine their results into a common conclusion and estimate, which at the same time includes

137 an estimation of their reliability: if the data contradict each other, the overall reliability will be lower. If they
138 support each other, the confidence interval will be smaller. And if there is no systematic bias that affects all
139 data sources to the same extent, it should be possible to arrive at the most reliable estimate possible through
140 the most heterogeneous set of data sources.

141 The well-established application of a Bayesian approach in radiocarbon calibration, where it is used to model
142 radiometric uncertainty based on stratigraphic information, represents a very similar use case in archaeology.
143 More recently, archaeologists have also used Bayesian modelling techniques as a tool for testing hypotheses
144 relating to demographic trends or underlying models based on ^{14}C data (e.g. Crema and Shoda, 2021).
145 This approach differs from the one presented in this paper in that, in these analyses, deductive models are
146 generated and their plausibility is tested on the basis of ^{14}C data only. This is a clear step forward in the
147 direction of a model-based, and thus scientific, analysis. However, the use of only one proxy, and its use
148 exclusively for testing hypotheses developed independently, creates problems comparable to those of the
149 inductive approaches used so far: due to the lack of a combination with other indicators, one is limited
150 to the problems and conditions of sum calibration as a tool. Furthermore, this approach loses significant
151 potential information that would be gained by a direct evaluation of the time series. Thus, the credibility of
152 a model can only be checked as a whole, without the dynamic developments that can arise in the course
153 of demographic processes being represented. We would like to better exploit the capabilities of Bayesian
154 hierarchical models through a combination of inductive data analysis and model-passed data integration of
155 different proxies.

156 Here, we attempt to make Bayesian hierarchical techniques usable for archaeological reconstructions. In
157 addition to a presentation of the basics and possible procedures, we want to show in the following, in a
158 reproducible and practical form using a case study, how Bayesian methods can also make a decisive contribution
159 to a better assessment of population development. These assessments are crucial for the reconstruction of the
160 human past, even in for periods for which we only have very patchy, noisy and unreliable data.

161 **2.3. Assumptions of a Bayesian approach**

162 The basis of Bayesian statistics is the premise that there is always some prior assumption about the probability
163 of an event, even if it may be very rough. This assumption is then adjusted by observing the data. The concept
164 of probability is not derived from theoretical, infinitely repeatable random experiments or distributions, but
165 from the direct confrontation of the pre-assumptions (priors) with the available data. This involves checking
166 how credible these prior assumptions are with regard to the available data (likelihood, see also Bryant and
167 Zhang, 2018, p. 66). A small amount of data leads to a broad probability distribution that is not strongly
168 localised and restricted. The intuitive procedure is thereby the shifting of credibility through evidence.

169 At the heart of all Bayesian statistics is therefore the concept of updating a given prior assumption with
170 new data and expressing this in probabilities (cf. also Kruschke, 2015, especially 15–25). Our assumptions
171 about the demographic development of the past must naturally be very conservative. In the logic of the basic
172 Bayesian equation, these assumptions represent the prior (probability). In conjunction with the data that
173 are included as the likelihood of the prior, a posterior (probability) results, which represents the Bayesian
174 model learning from data. It is also in the nature of the approach that in real applications there is no point
175 prediction, but in most cases a probability distribution for the prediction. Thus, we simultaneously obtained
176 a result and an estimate of the confidence intervals, or rather the credibility interval, given the data.

177 This Bayesian learning is iterative and sequential, so that the result of one Bayesian inference can form the
178 prior of another, i.e. it is an additive process (Kruschke, 2015, p. 17). Moreover, at the conceptual level,
179 this allows different sources of information to be combined (Bryant and Zhang, 2018, pp. 219–224). This
180 enables that they can be mapped to the same set and the same real-world domain, e.g. probabilities. This
181 fact has long been exploited by archaeology in using stratigraphic information to make radiometric dating
182 more accurate (Ramsey, 1995). ^{14}C dates and stratigraphy are something completely different, but both can
183 be mapped to the probability of older and younger and combined in this way. The same is also feasible when
184 it comes to the probability of population sizes or population densities or their derived dynamics.

185 A further characteristic of Bayesian modeling is that, due to the fact that results of a Bayesian inference can
186 be regarded as a prior for the next one, a hierarchical formulation of problem domains is possible. Parameters

187 that are necessary for an estimation, such as the relationship of population density to the deforestation
188 signal in pollen data, need not be specified explicitly, but can be given by probability distributions and then
189 estimated in the model itself (Bryant and Zhang, 2018, p. 186). The more data available, the more degrees
190 of freedom can be estimated with a reasonable loss of confidence or a reasonable width of credibility intervals
191 (Kruschke, 2015, p. 112). For the estimation of these parameters, in turn, submodels have to be created
192 which describe the relationship of the data to the characteristics of the parameter. This can be carried out
193 over several levels, depending on necessity (Kruschke, 2015, pp. 221–222).

194 3. Materials: Population proxy data

195 The case study area north of the Swiss Alps (Figure 1) covers about one third of Switzerland's territory and
196 comprises the partly flat, but largely hilly area, between the Jura Mountains and the Alps. It averages an
197 altitude of between 400 and 600 m a.s.l. It is a favourable area for settlement and agriculture and especially
198 the Swiss Plateau is by far the most densely populated region of the Switzerland today. The Swiss Plateau
199 between Lake Zurich and Lake Geneva will serve as a core region in our case study, because archaeological
200 data from there is most abundant and accessible. Although it is a basin, depending on the region it has a very
201 diverse natural landscape: shaped by glaciers during the ice ages, the many lakes and bogs that characterise
202 the landscape today also provide excellent preservation conditions for the numerous Neolithic and Bronze
203 Age lakeside settlements, as well as a rich pool of sources for vegetation reconstructions by means of pollen
204 analyses. Thanks to the very active and efficient archaeological research and heritage management there is an
205 abundance of archaeological information, including known sites as well as dendrochronological and ^{14}C data.

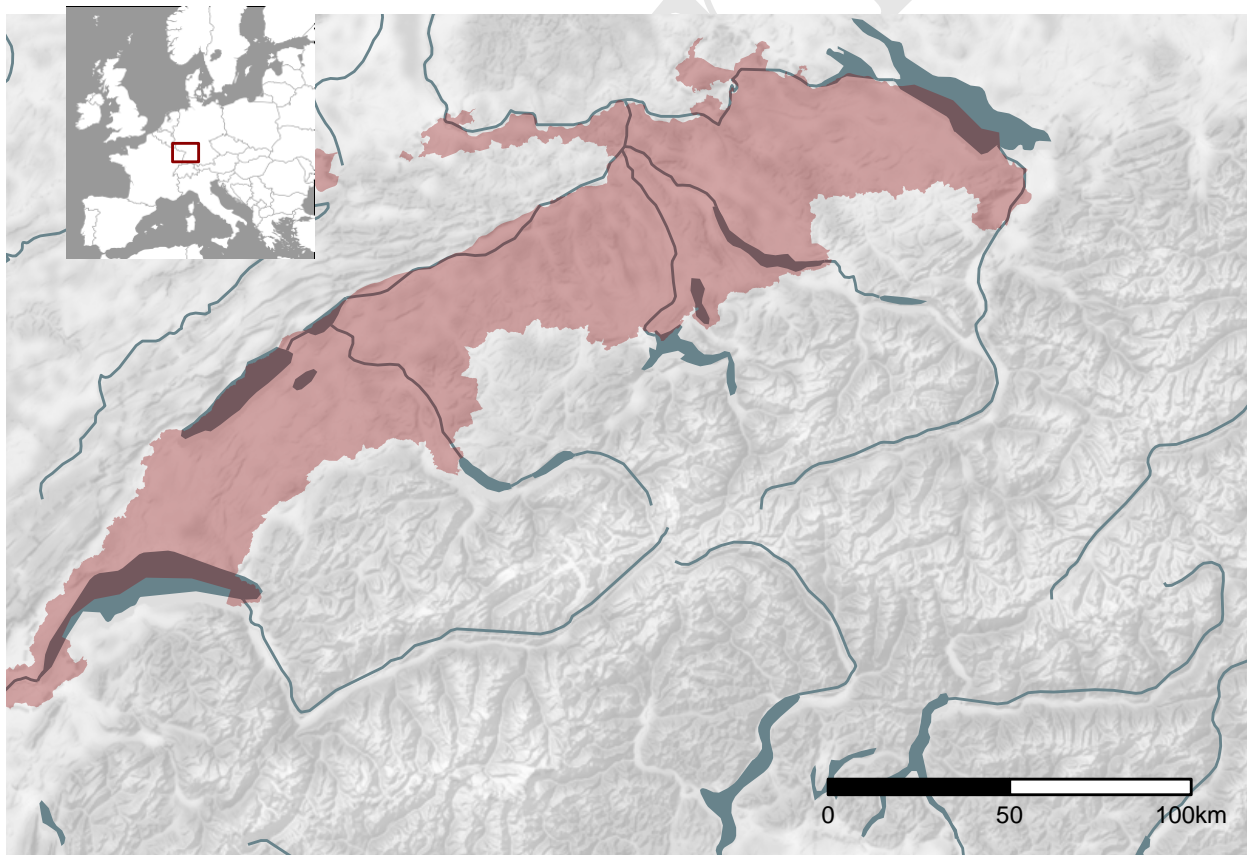


Figure 1: Location and extent of the Swiss Plateau as biogeographical region (based on swisstopo) including additional low altitude areas in the north of Switzerland (regions along the High Rhine between Schaffhausen and Basel).

- 206 Our case study targets the period between 6000–1000 BCE. The lower limit of this window was chosen to
 207 avoid the so-called ‘Hallstatt plateau’ on the Northern Hemisphere radiocarbon calibration curve, which
 208 would cause difficulties for the ^{14}C proxy data. The upper limit was chosen to coincide with post-glacial
 209 changes in pollen spectra, before which the openness indicator is highly unlikely to reflect human influence
 210 before 7000 in the working area.
- 211 In principle, a large number of different data sources can be integrated into the overall model as proxies,
 212 provided that these observations a) can be understood as dependent on the population density in the past,
 213 and b) a model-like description of this dependence can be created. Table 1 provides a non-exhaustive list.
 214 For our case study, we used: a landscape openness indicator; an aoristic sum of sites based on typological
 215 dating; a sum calibration; and frequency data for dendro-dated lakeshore settlements in the Three Lakes
 216 region (western Swiss Plateau).

Table 1: A incomplete list of possible observation that can be linked
 to population developments in the past. Proxies used in this study
 are highlighted.

Proxies
Expert estimates
Ethnographic Analogies
Carrying Capacity
Economic modelling
Extrapolation of buried individuals
Burial anthropology
Settlement data, number of houses
Settlement data, settlement size
Aoristic analysis
Dendro dates
Amount of archaeological objects
Radiocarbon sum calibration
Estimates based on specific object types
Human impact from pollen or colluvial data
aDNA based estimates
...

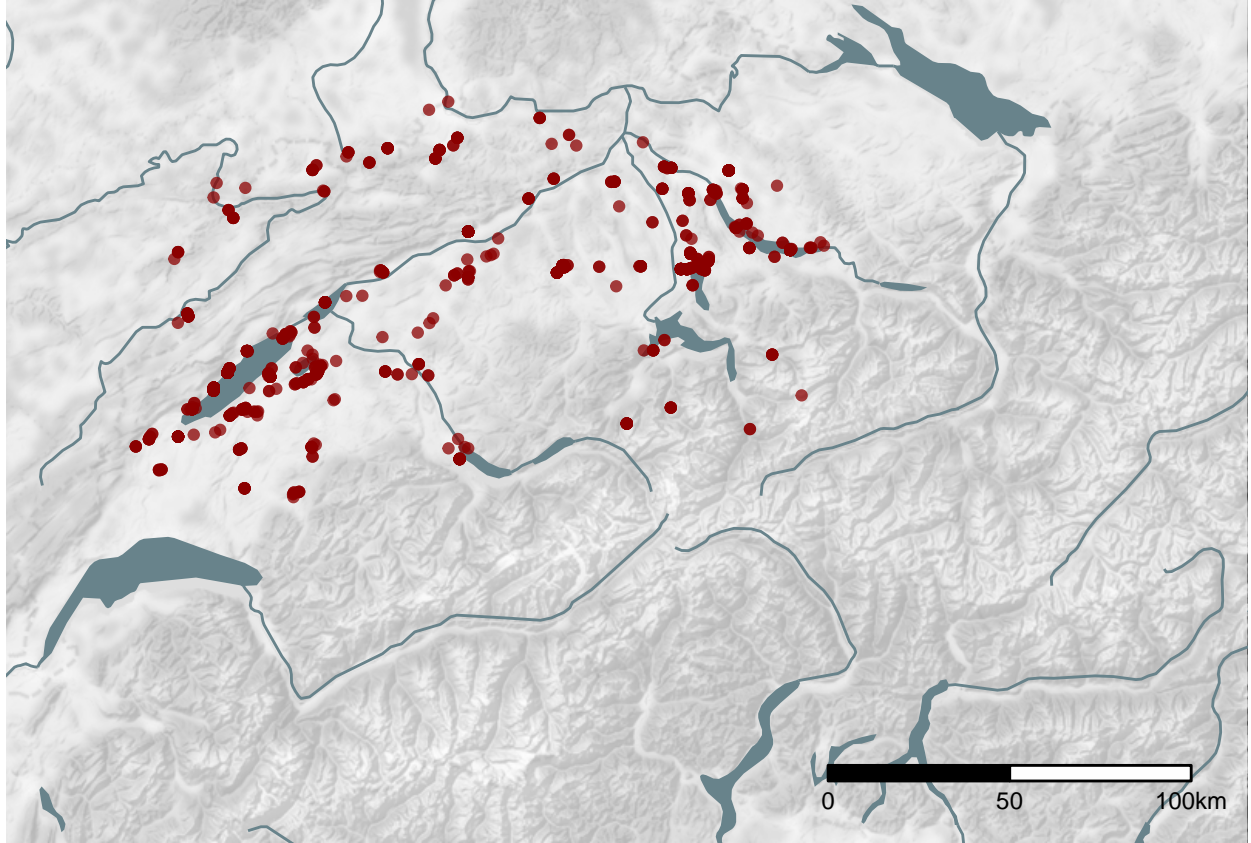
217 3.1. Dendro-dated lakeshore settlements

- 218 With the vast areas of arable soils with small slope gradient compared to the Jura and the Alps, and a
 219 dense network of water bodies, the Swiss Plateau has always been a particularly favourable area for human
 220 settlement in Switzerland. From the Neolithic onwards, settlement areas were concentrated along its rivers
 221 and lakes (Christian Lüthi, 2009). Thus, our working region offers on the one hand excellent data for
 222 demographic estimation, but on the other hand poses very specific problems for such an undertaking. If
 223 we have high-resolution information on the temporal sequence of individual settlements at the lakeside
 224 settlements by means of dendro data, this also might cause a research problem with regard to the ^{14}C data
 225 often used as a proxy.
- 226 The dataset we use for the number of dendro-dated wetland settlements in the Three Lakes region was
 227 collected by Julian Laabs for his PhD thesis (Laabs, 2019). Details on the creation of this data series will be
 228 published at the referenced location. The time series used here runs from 3900 to 800 BCE, and contains the
 229 number of chronologically registered fell phases at individual settlements. This results in a time series that
 230 reflects the settlement of the lakeshores in the Neolithic and Bronze Age periods.

231 3.2. Summed radiocarbon

232 The dataset for the ^{14}C sum calibration primarily consists of data from the XRONOS database (<https://xronos.ch>), supplemented by dates from the unpublished PhD thesis of Julian Laabs (Laabs, 2019) and the
233 data collection of (Martínez-Grau et al., 2021). It contains a total of 1135 single ^{14}C data from 246 sites. The
234 dates were selected so that their distribution area coincides with the catchment area of the pollen proxy (see
235 also Figure 2). The dates in the dataset range in ^{14}C years from 10730 to 235 uncal BP. This time window
236 extends beyond the study horizon in order to minimise boundary effects.

237 We binned the data at site levels to obtain a temporally dispersed count and thus an expected value of
238 contemporaneous ^{14}C dated sites. For the creation of the cumulative calibration, the corresponding functions
239 of the R package rcarbon (Crema and Bevan, 2021) were used with their default settings.



240 Figure 2: The location of the ^{14}C dated sites in the dataset.

241 We can now compare these two data sets (Figure 3). In fact, there is a not uninteresting fit between the two
242 data series. However, it must be assumed that the two dating methods, even if they would contradict each
243 other, actually complement each other, and thus allow a better overall unified picture of the actual settlement
244 density than each of the individual proxies would allow on their own.

245 3.3. Aoristic sum

246 To add another archaeological indicator of occupation, we include relative dating information obtained from
247 the Swiss cantonal archaeology/heritage management authorities (Figure 4). These are primarily derived
248 from scattered surface finds, which often have a low dating accuracy. We incorporate this data into our model
249 as a typologically dated aorist time series. The dating accuracy is only in the range of archaeological periods,
250 but the advantage is that we are not bound to the conditions and problems of radiocarbon dating and thus
251 methodological issues of sum calibration can be avoided. Furthermore, this data provides an independent

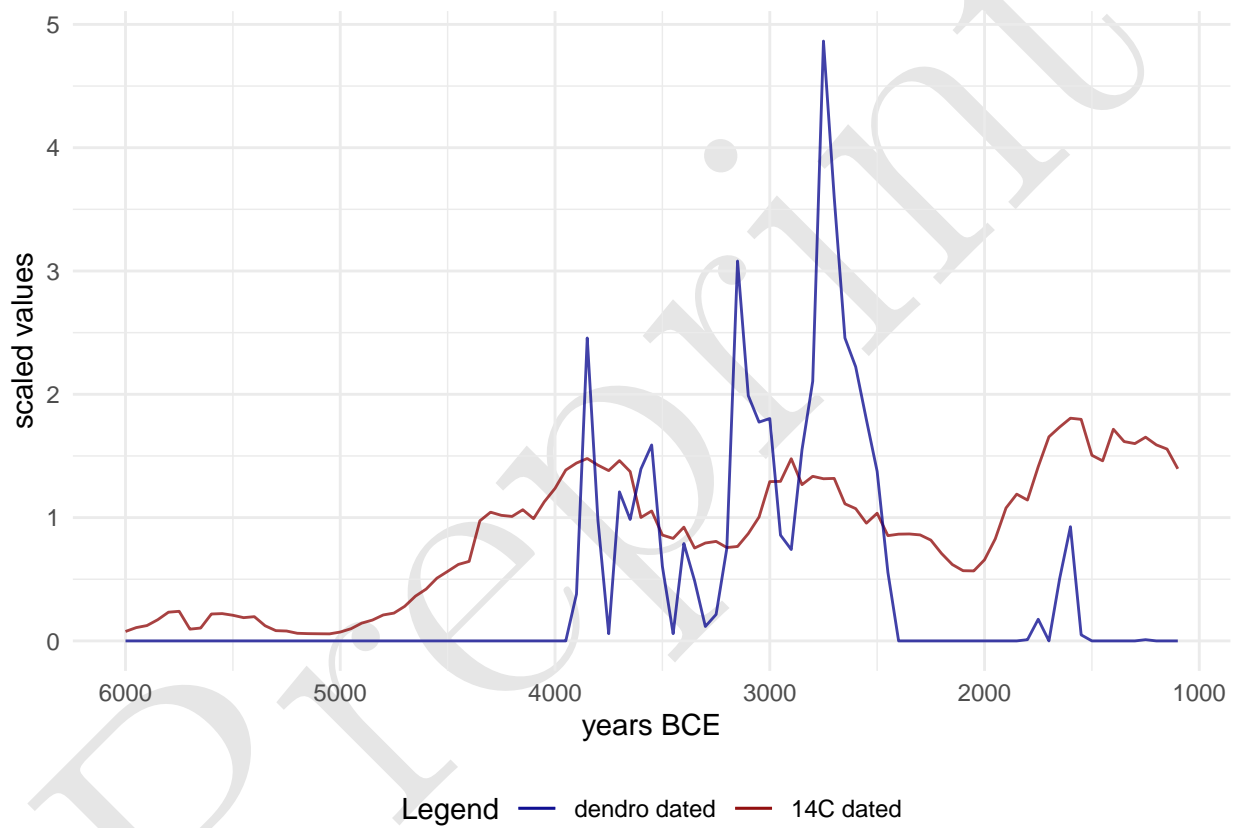


Figure 3: Comparison of the scaled (non-centered z-transformed) number of ^{14}C and dendro-dated sites over time in the dataset used.

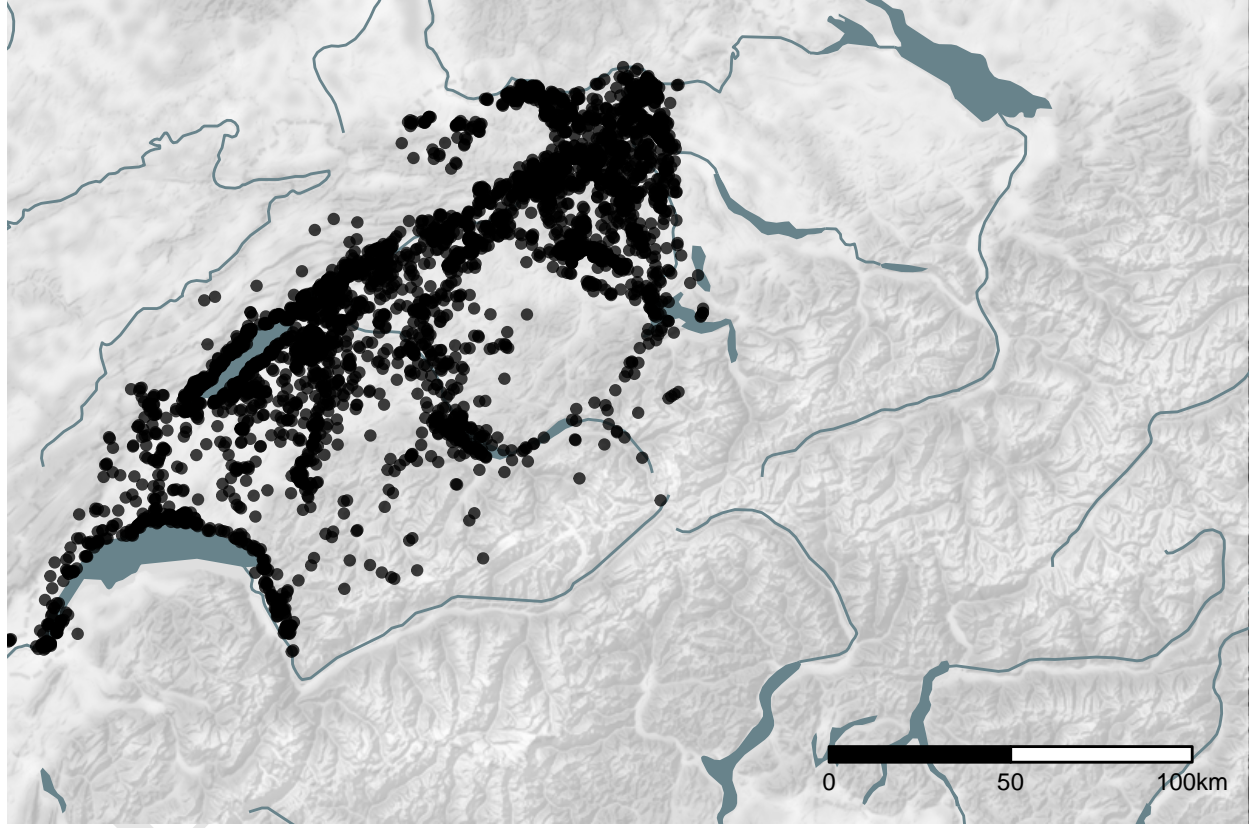


Figure 4: The location of the sites from the find reports of the cantonal archaeology (heritage management). The locations are ‘fuzzed’ by ~1km.

252 indicator with regard to the methodology of the ^{14}C data, even if they are influenced by similar transmission
 253 filters and archaeological conditions as the evaluation of ^{14}C data. Data from 4321 sites were included in the
 254 aoristic sum, which is a very rough indicator due to the low dating accuracy offered by archaeological phases,
 255 but which nevertheless has an important role in the normalisation of the data due to its independence from
 256 calibration effects.

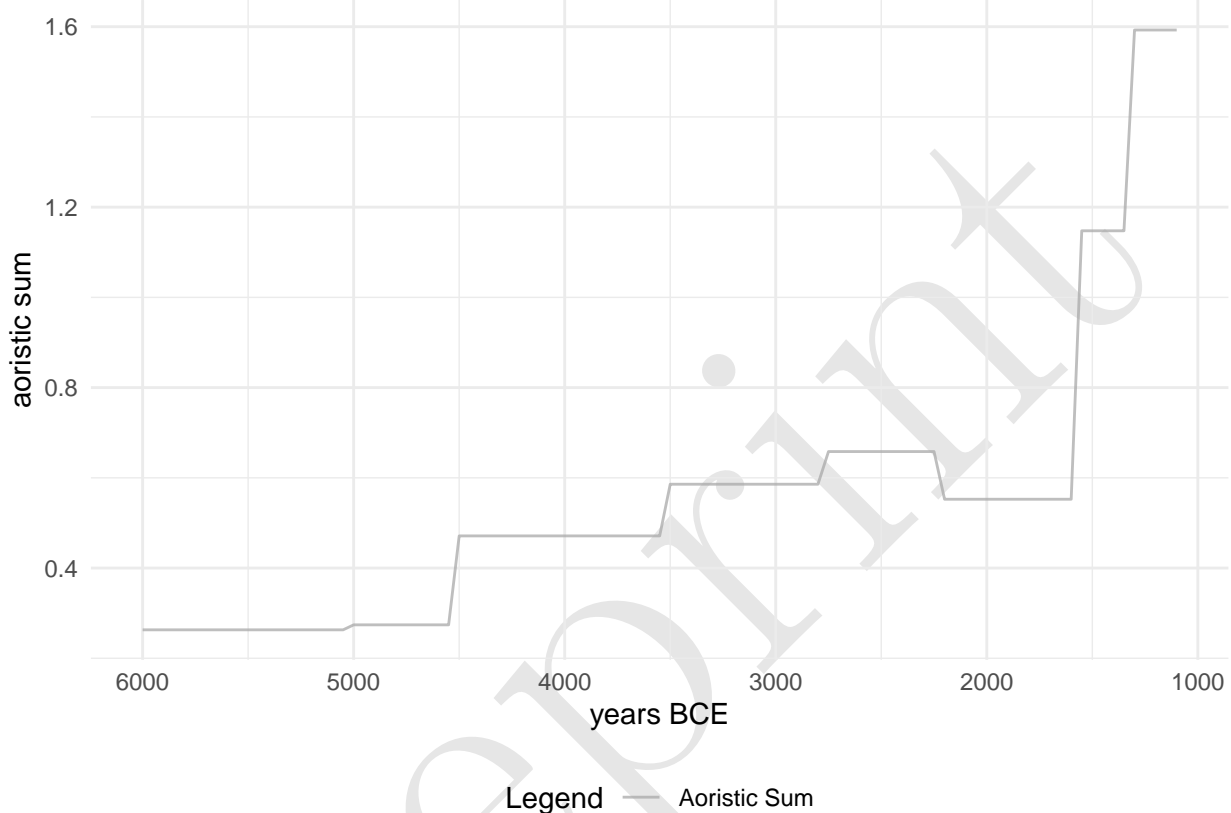


Figure 5: Aoristic sum of the archaeological sites used in this analysis.

257 **3.4. Landscape openness**

258 The natural conditions of the lakes of the Swiss Plateau enable not only highly precise dating of archaeological
 259 sites, but also a very dense network of pollen analysis. We make use of this fact by generating a supra-
 260 regional openness indicator for the vegetation from the pollen data (Figure 6). This proxy has the specific
 261 advantage that it is not dependent on preservation conditions, as archaeological indicators are. This makes it
 262 particularly valuable for indicating or compensating for systematic distortions that result from temporally
 263 specific settlement patterns and archaeological preservation conditions.

264 The utilisation of this proxy is based on the assumption that the higher the population density in an area, the
 265 greater the human influence on the natural environment (Lechterbeck et al., 2014), and that the extensiveness
 266 of agricultural activity in an area is related to human population density (Zimmermann, 2004). Evidence of
 267 land clearance in pollen diagrams can therefore provide further indications of population dynamics where
 268 humans can be assumed to be the main driver of this process, which is the case in much of Europe. The full
 269 procedure for deriving this proxy from several different pollen diagrams is detailed in a previous publication
 270 (Heitz et al., 2021). In this study, five pollen diagrams from sites mainly in the hinterland of the large
 271 Alpine lakes were used. The technical steps are also documented in the accompanying R compendium. The
 272 percentage pollen data, based on a pollen sum of all terrestrial taxa of the individual sites, was combined
 273 into one data set by means of a principal component analysis (Figure 7). Only terrestrial pollen taxa
 274 with a frequency of more than one third and, if present, with an average frequency of at least 0.1% were

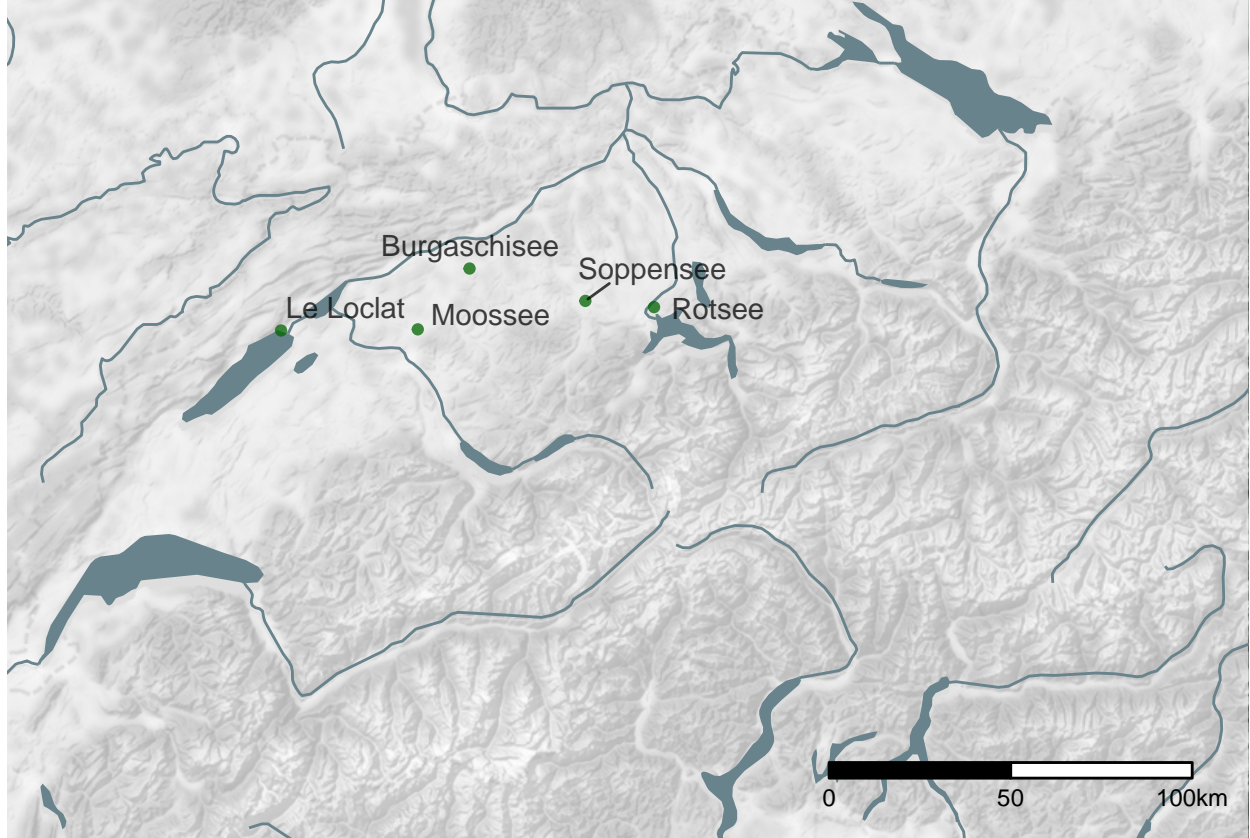


Figure 6: Location of the pollen profiles used for the openness indicator.

275 selected to reduce potential disturbance by rare species. Cereal pollen was explicitly retained as an important
 276 anthropogenic indicator. As each sample is absolutely dated, the data on the x-axis can be plotted against
 277 the openness value on the y-axis to obtain a time series time series for land clearance.

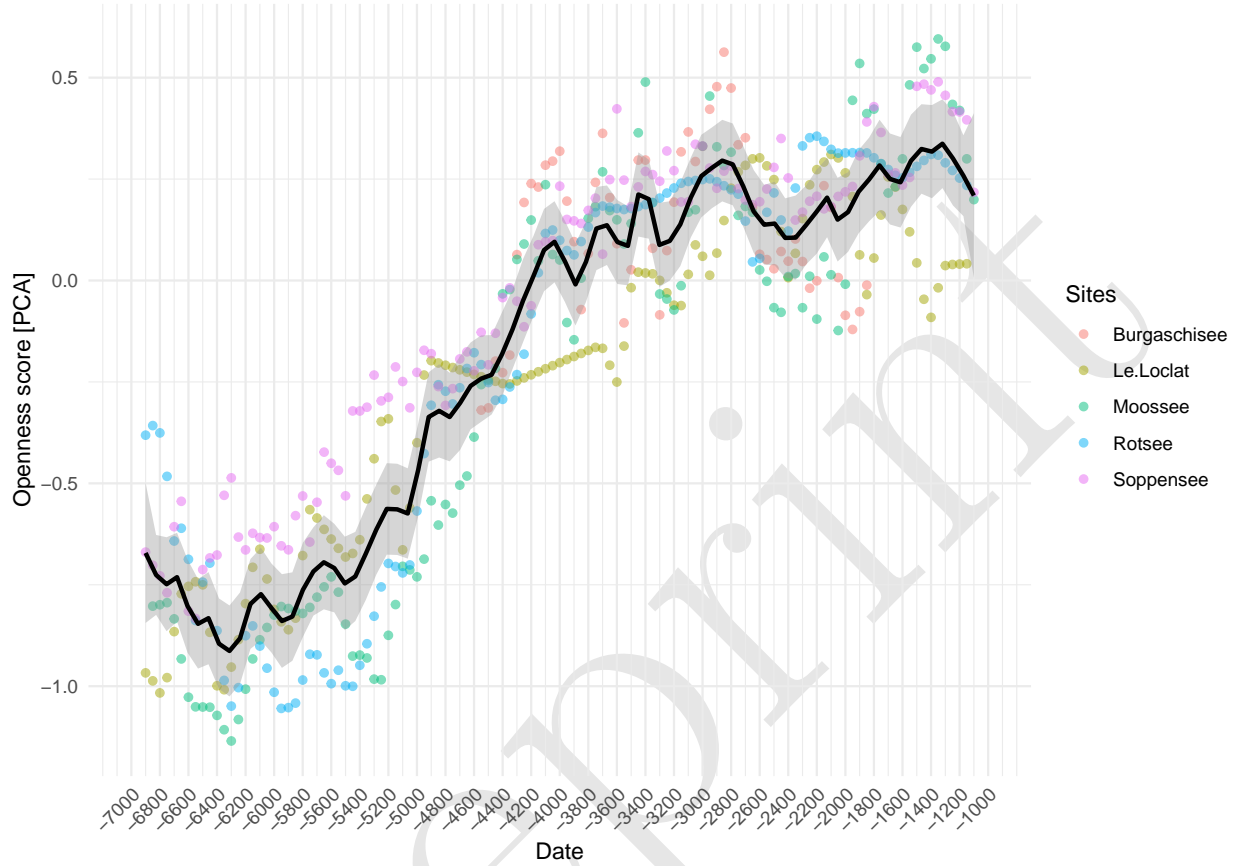


Figure 7: Value on the first dimension of the PCA against dating of the samples for the individual pollen profiles and their combined average value as the openness indicator.

278 3.5. Other proxies

279 Unfortunately, there is no burial data available in the case study area that could be usefully incorporated
 280 into such this model due to the absence of regular burials for larger parts of prehistory. Formation conditions,
 281 in this case most likely C-transformation (Schiffer, 1987), the active cultural choice to not use archaeological
 282 traceable burial pratices, prevent their use in this study. Nevertheless, we see a very high potential for other
 283 regions in the integration of demographic indicators from burial data in order to enlarge the canon of methods
 284 and the range of proxies.

285 4. Methods: Bayesian model

286 The sum calibration, openness and the dendro-dated settlement data was smoothed by means of a moving
 287 average with a window of 50 years. The aoristic sum was not smoothed, because it already has a very coarse
 288 temporal resolution. The range of the smoothing window corresponded to the sample interval, with which a
 289 unified resolution of 50 years was obtained for all proxies as time slices for the model. In addition, all data
 290 was restricted to the window of observation of 7000–1000 BCE.

291 In the construction of our ‘observational model’, we considered all these proxies as informative of the number

292 of settlements located in the north of the Swiss Alps. Consequently, we shift the causality and consideration
293 of measurement error, which is certainly inherent in each of these proxies, to a preceding ‘process model’,
294 in which a Poisson process describes the number of simultaneous settlements. In doing so, we establish a
295 likelihood that estimates how credible the data is, given the model.

296 4.1. Process model

297 A special class of Bayesian hierarchical models are so-called State Space Models (also known as Hidden
298 Markov Models). These are specifically designed for time series and follow two basic principles. First, a
299 hidden or latent process is assumed, which represents the state of the variable of interest x_t through the
300 entire time series. Over time, it is assumed that every state of variable x in the future, as well as in the past,
301 is bound by a Markov process to the state of variable x at time t . At the same time, it is assumed that
302 certain observations, represented in variable y , are dependent on the state of variable x at time t . This means
303 that there is a relationship between the variable x and the state of variable y over time. This implies that
304 a relationship between the individual states of variable y is generated over time via the hidden variable x ,
305 which itself is not observable.

306 This basic structure of this class of model makes it particularly useful and suitable for the purpose of
307 demographic reconstruction using archaeological and other data which are reflective of population density in
308 the past. This population density itself is not accessible or measurable by our means. All we have at our
309 disposal are observations derived by unknown transfer functions. These can be of very different natures, such
310 as number of archaeologically observable settlements, or other effects that can be observed through time
311 series, and which are influenced by population in a given area. In our case study, these are the openness
312 indicators from pollen data, which we can interpret primarily in terms of human influence and its intensity.
313 On a more abstract level, we could also include expert estimates, as these also happen on (often unspecified)
314 bases that are at least indirectly influenced by past population density.

315 The overall model for the estimation of demographic developments is broken down into several hierarchically
316 interconnected individual elements in accordance with the basic structure of a state space model. The basis
317 is a process model that represents the demographic development itself in terms of a structure model, without
318 this model already being explicitly configured with data.

319 In this process model we assume that the latent variable ‘number of sites’ is strongly autocorrelated across
320 different time periods, i.e. the number of sites in 3000 BCE is strongly conditioned by the number of sites
321 in 3050 BCE, and so on. In principle, one can represent a population development in such a way that the
322 population at time t results from the population at time $t - 1$ times a parameter λ , which represents the
323 population change at this time. This gives us the basic formula:

$$N_t = N_{t-1} * \lambda_t$$

324 The Poisson distribution is particularly suitable for modelling frequencies. It is a univariate discrete probability
325 distribution that can be used to model the number of events that occur independently of each other at a
326 constant mean rate in a fixed time interval or spatial area. It is determined by a real parameter $\lambda > 0$, which
327 describes the expected value and simultaneously the variance of the distribution. Thus, the relationship
328 shown above can also be rearranged as follows:

$$\begin{aligned} N_t &\sim dpois(\lambda_t) \\ \lambda_t &= N_t \end{aligned}$$

329 If we now have information about the change in population development (the proxies), we can use this to enter
330 it into the model via a change in λ . This is done in the form of a regression: for all proxy values—represented
331 as a vector of independent variables $x \in R^n$, with R^n as an n -dimensional Euclidean space, described in this
332 case by the n dimensions of the n variables—then the model takes the form:

$$\log(E(Y | x)) = \alpha + \beta'x$$

333 Using the logarithm as a link function ensures that λ , which must always be positive for a Poisson process,
 334 can also be described by variables (proxies) that range in the space of real numbers and can therefore also be
 335 negative. β can serve here as a slope factor, just as in a normal linear regression. In our case, it functions as
 336 a scaling factor for the individual proxies. α , is to be understood as an intercept. If there were no change due
 337 to the variables, the regression would fall back to this value. This corresponds to the desired behaviour. In
 338 the case of population trends, the intercept would be equal to the value of the population in the previous time
 339 period, plus or minus the changes resulting from the variables. If there is no change from these variables, then
 340 λ , and thus the expected value for the current time step would be equal to that from the previous time step:

$$\log(\lambda_t) = \log(N_{t-1}) + \sum_{i=1}^n \beta_i x_{t,i}$$

341 Since λ and N are essentially in the same range (e.g. if $lambda = 1$, the expected value for N would also be
 342 1), N_{t-1} must also be log-transformed in the above formula to obtain the congruence of both values. The
 343 values for population size N_t as well as for population change λ_t are time-dependent. At each individual
 344 point in time in the time series, these variables can or will also take on different values. However, we can
 345 narrow down the structure of population change even further. We can assume that, considered overall over
 346 time, the population change will not exceed certain limits over the entire timespan, though it is not possible
 347 to specify this at this point.

348 Thus, we can define the limits, the *max_change_rate* as a time independent variable, again without specifying
 349 them with fixed values at this stage. The estimation of these parameters for the entire model, as well as
 350 the estimation of the respective population change per time section, results from the modelling and the
 351 interaction with the data, respectively. Overall, this represents a hierarchical model that can be noted as
 352 follows:

$$\begin{aligned} max_growth_rate &\sim dgamma(shape = 5, scale = 0.05) \\ N_t/N_{t-1} &< (max_growth_rate + 1) \\ N_{t-1}/N_t &< (max_growth_rate + 1) \end{aligned}$$

353 The gamma distribution used centres the probability in a range $[0, 1]$, adding 1 makes this range $[1 - 2]$.
 354 This prevents the number of sites from explosively increasing between two time periods, which would be
 355 unrealistic given our sampling interval (50 years), and would lead to problems for the convergence of the
 356 model. The interaction of these parameters results in the following prior probability distribution for λ and
 357 thus the growth (or change) rate of the population.

358 4.2. Observational model

359 During the development of our model, we experimented with but ultimately abandoned the idea of implementing
 360 dedicated observation models adapted to the conditions of the individual proxies and their generating
 361 processes. We found that underdetermination of currently usable data in the model, having many degrees of
 362 freedom, produced a high degree of equifinality in the solutions and thus led to a high path dependency in
 363 individual model runs. As a result, it was almost impossible to achieve convergence of the overall model.
 364 Nevertheless, we believe that in future applications of the model with more data, a larger geographical
 365 coverage and/or, especially, a regionalised approach with information transfer by means of partial pooling,
 366 this more specific approach would be a feasible and a very useful approach.

367 The implementation we present in this paper instead represents a Poisson regression, where the proxies are
 368 used to inform the change in the number of settlements from time step to time step. For this purpose, the
 369 individual proxies were z-normalised. The absolute differences from one time step to another were then

370 computed from the resulting time series. Thus, if the value of the proxy increases, this results in a positive
 371 difference from the previous time step, and vice versa.

$$z_t = \frac{x_t - \bar{x}}{\sigma_x} \mid \sigma_x := \text{Standard Deviation}$$

$$\delta z_t = z_t - z_{t-1}$$

372 The sum of the resulting differences between the time steps, together with the settlement number of the
 373 previous step as the expected value, then forms λ_t as the expected value for the settlement number of the
 374 current time step.

$$\log(\lambda_t) = \log(N_{t-1}) + \sum_{i=1}^n \beta_i \delta z_{i,t}$$

375 Here, β_i is a scaling factor that represents the influence of the respective proxy. It is a confidence value of the
 376 model for the respective proxy, so that the sum of all β_i results in 1.

$$\sum_{i=1}^n \beta_i = 1$$

377 A probability distribution that can be used for this purpose in a hierarchical Bayesian model is the Dirichlet
 378 distribution, which is a multivariate generalization of the beta distribution, commonly used as prior distribu-
 379 tions in Bayesian statistics. Its density function gives the probabilities of i different exclusive events. It has a
 380 parameter vector $\alpha = (\alpha_1, \dots, \alpha_n) \mid (\alpha_1, \dots, \alpha_n) > 0$, for which we have chosen a weakly informative log-normal
 381 prior. The priors for the log-normal distribution in turn come from a weakly informative exponential
 382 distribution for the mean and a log-normal distribution with μ of 1 and σ_{\log} of 0.1:

$$\begin{aligned}\beta_i &\sim Dir(\alpha_{1-i}) \\ \alpha_i &\sim LogNormal(\mu_{alpha_i}, \sigma_{alpha_i}) \\ \mu_{alpha_i} &\sim Exp(1) \\ \sigma_{alpha_i} &\sim LogNormal(1, 0.1)\end{aligned}$$

383 As an intuition, this means that we consider the sum of the proxies as determinant for the number of
 384 settlements. The estimation therefore assumes that all proxies together give the best possible estimation
 385 result for contemporaneous sites at time t , whereby the share of each individual proxy is considered variable
 386 and is estimated within the model. This share is recorded within the model as the parameter p .

387 The error value is represented by the Poisson process in the process model, rather than directly as an
 388 estimation error for the individual proxies. Thus, our model does not correspond to a classical state space
 389 model, where the measured values are each considered to be error-prone. In the implementation, the model
 390 finds the best possible combination or compromise between the individual proxies to describe a settlement
 391 dynamic that is given by them. In addition, the number of sites is converted into population density using
 392 some (certainly debatable) parameters that we have defined but which are only scaling factors for the
 393 intermediate value of number of settlements. For this, we assume that each site represents a number of people
 394 that is poisson distributed around the value 50. The number 50 represents a compromise, as both Mesolithic
 395 and Neolithic and Bronze Age settlement communities need to be represented. By means of a data series,
 396 which would represent an evidence-based estimate of the temporal development of settlement sizes, this
 397 specification could be made based on data. From the number of sites and the mean number of individuals
 398 represented in each case, a population density can be calculated using the case study area (12649 km^2). The
 399 estimated result of the model is thus comparable with estimates from other sources or the literature.

400 In earlier implementations, expert estimates were also integrated into the model. However, since these are
 401 highly contradictory for the working area (Figure 8, we found they had little influence on the model and also

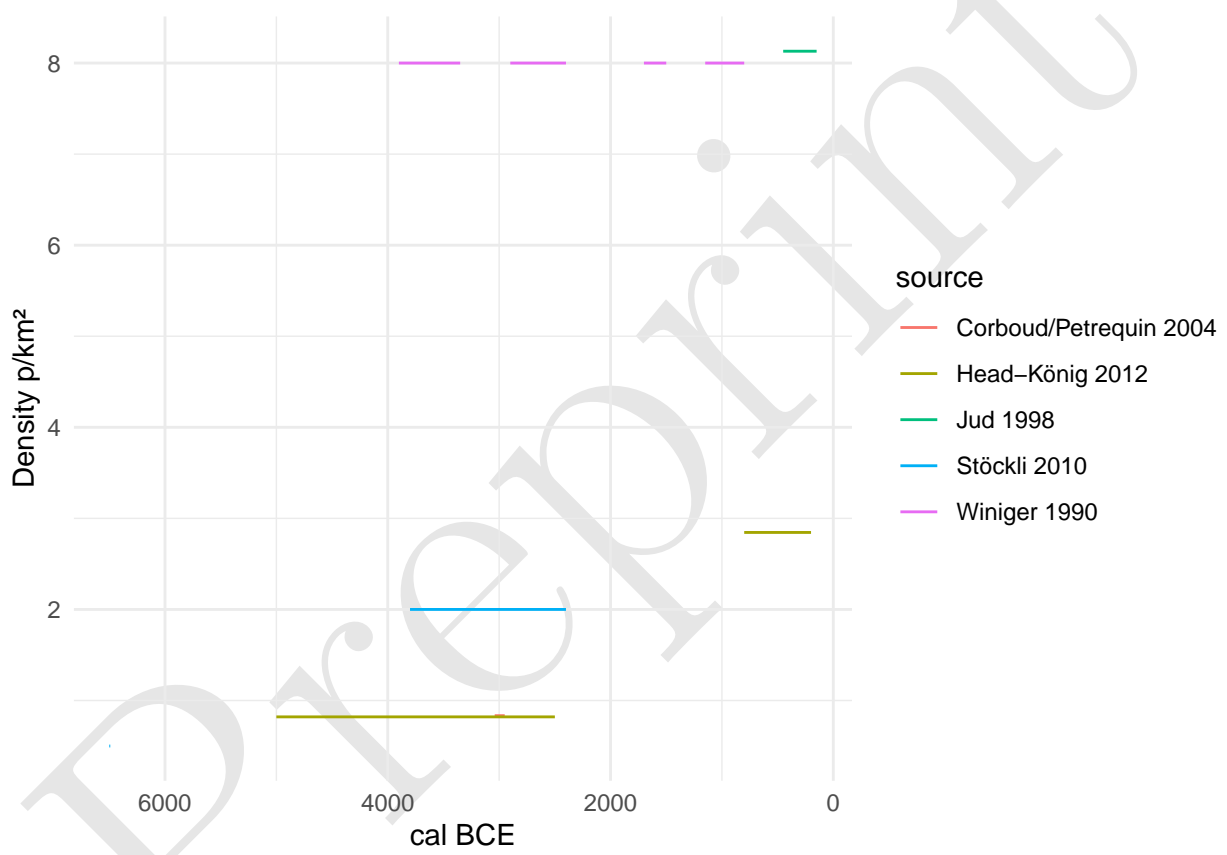


Figure 8: Expert estimations for the population density on the Swiss Plateau from different authors.

402 significantly increased its runtime. We therefore excluded them in the implementation presented here, but
 403 again, given a larger geographical range and thus a higher information density, this proxy could be usefully
 404 integrated into future applications.

405 4.3. Model fitting

406 The model was fitted using the R package *nimble* (version 0.11.1, R version 4.1.3). For this purpose, 4 chains
 407 were run in parallel. Achieving and ensuring convergence and sufficient effective samples (10000) for a reliable
 408 assessment of the highest posterior density interval was carried out in steps.

409 In a first run, the model was initialised for each chain and run for 100000 iterations (with a thinning of
 410 10). On a reasonably capable computer (Linux, Intel(R) Xeon(R) CPU E3-1240 v5 @ 3.50GHz, 4 cores, 8
 411 threads), this takes approximately a minute.

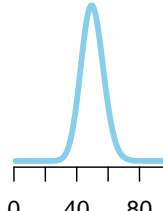
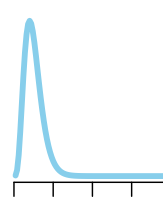
412 In a second step, the run was extended until convergence could be determined using Gelman and Rubin's
 413 convergence diagnostic, the criterion being that a potential scale reduction factor of less than 1.1 was achieved
 414 for all monitored variables. Convergence occurred after about thirty seconds.

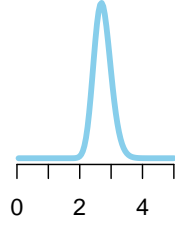
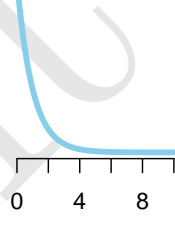
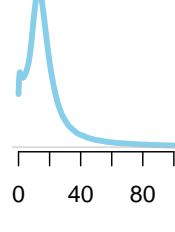
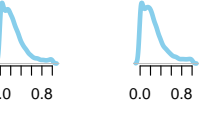
415 Due to the high correlation of the parameters and thus a low sampling efficiency, the collection of at least
 416 10,000 effective samples for all parameters in the third step took about five hours.

417 For the fitting process, a starting value of 5 p/km² for a population density of the Late Bronze Age (1000
 418 BCE) was taken from the literature, which may represent a general average value for all prehistoric population
 419 estimates (Nikulka, 2016, p. 258). For the model, this was set as the mean of a normal distribution
 420 with a standard deviation of 0.5, which should give enough leeway for deviations resulting from the data.
 421 Nevertheless, especially the late part of the reconstruction is of course clearly influenced by this predefined
 422 value.

423 For the traceplots and the prior-posterior overlap as well as the density functions of the posterior samples of
 424 the individual parameters, please refer to the supplementary material.

Table 2: Priors and fixed parameters used in the model.

Priors	Value	Plot/Comment
MeanSiteSize	dpois(50)	 A density plot showing a single sharp peak centered around 50. The x-axis ranges from 0 to 100 with major ticks at 0, 40, 80.
max_growth_rate	dgamma(shape = 5, scale=0.05) + 1	 A density plot showing a single sharp peak centered around 1.0. The x-axis ranges from 1.0 to 3.0 with major ticks at 1.0, 2.0, 3.0.

Priors	Value	Plot/Comment
mu_alpha	dlnorm(1,sdlog=0.1)	
a_alpha	dexp(1)	
alpha	dlnorm(mu_alpha[j],sdlog=a_alpha[j])	
p	ddirch(alpha[1:4])	
Parameters		
nEnd	5	
AreaSwissPlateau	12649 km ²	
Initial Values		
lambda _{1:nYears}	$\log(1 - 10^{\frac{1}{nYears-1}})$	exponential increase of the factor 10
PopDens _{1:nYears}	nEnd (=5)	
nSites _{1:nYears}	50	

425 5. Results

426 The population density estimated by the model (Figure 9) ranges on between 0.2 p/km² for the beginning of
 427 the estimate (6000 BCE) and 4.8 p/km² for the end of the estimate (1000 BCE), reaching a maximum of 6.5
 428 p/km² for the time slice 1250 BCE. Thus, the estimate remains within the values that are also considered
 429 plausible by the expert estimates. Clear peaks are reached around 1250 BCE, as well as around 2750 BCE,

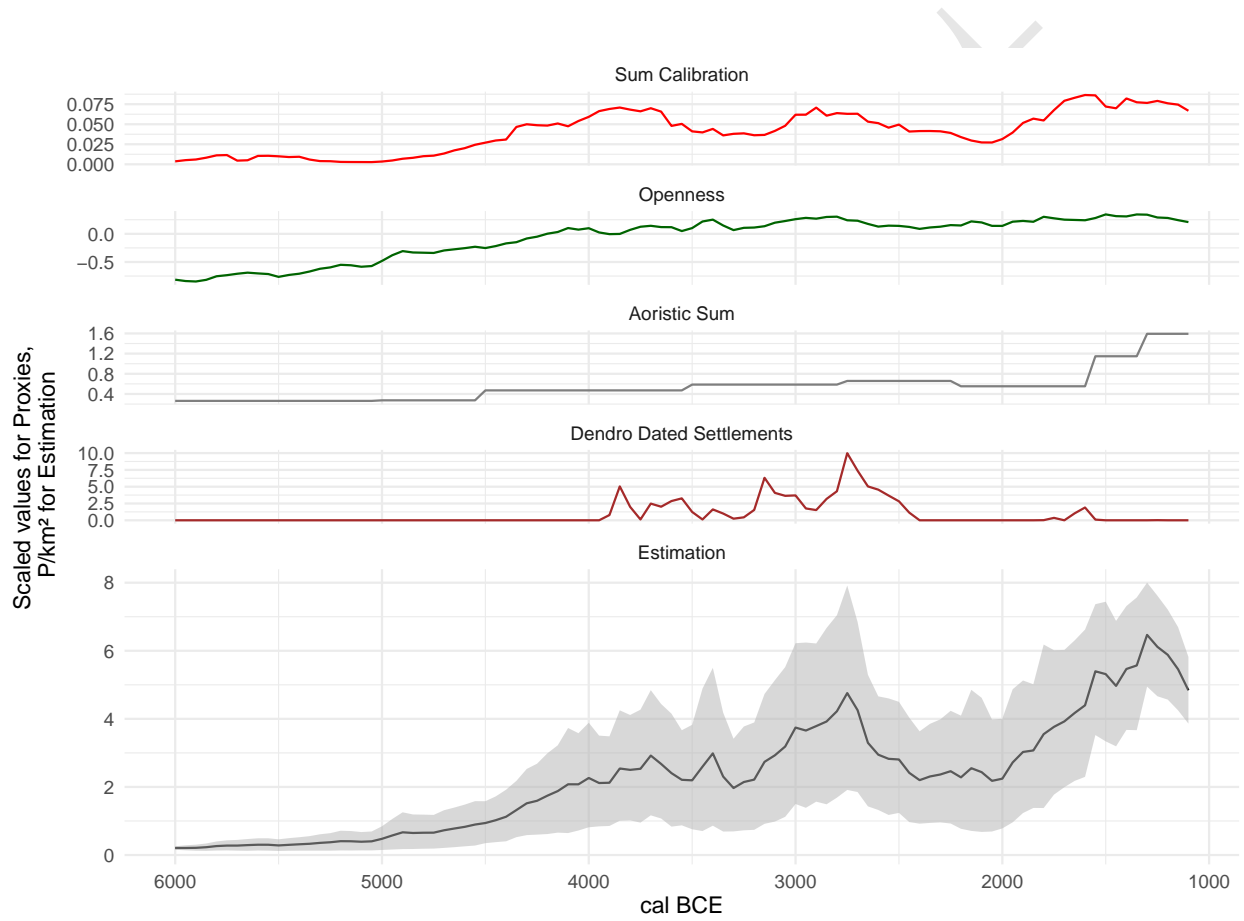


Figure 9: The estimate of the population density resulting from the model and the four proxies, which are also plotted (scaled) for comparison.

430 which corresponds to the transition to a ceramic style as observed for sites of the Swiss Plateau influence by
 431 the Corded Ware ceramic style (Hafner, 2004).

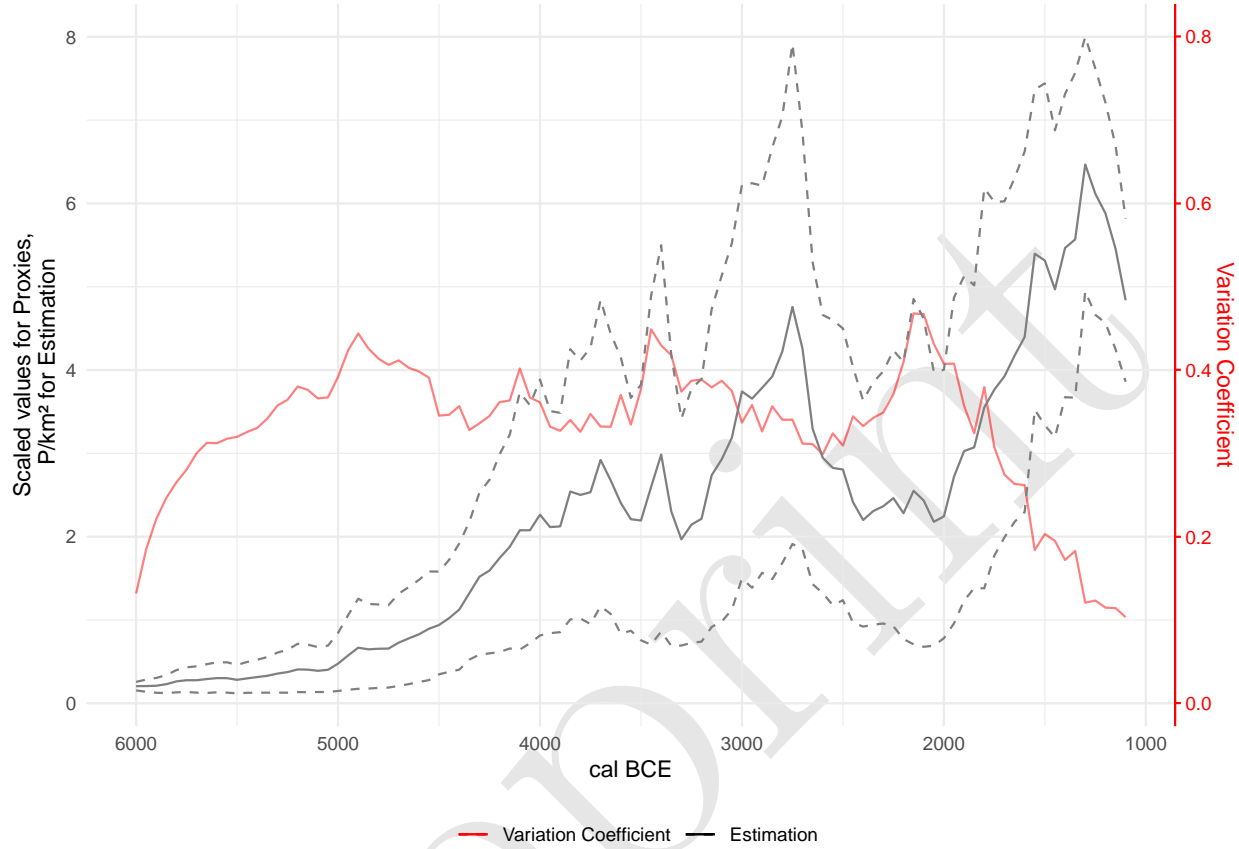


Figure 10: The variability of the estimate of the population density over time, with the estimate itself for reference.

432 The temporal distribution of the variability in the estimate (Figure 10) allows us assess at which time steps the
 433 model attempts a more accurate estimate, and at which the uncertainty is greater due to e.g. contradictions
 434 in the proxies. The coefficient of variation is 0.13 for the beginning and 0.1 for the end of the estimate,
 435 the greatest variability is reached around 2150 BCE with 0.47. This is not astonishing as there are fewer
 436 archaeological contexts recorded connected to the earlier phase of the Early Bronze Age c. 2200-1800 BCE,
 437 this picture changes from c. 1800 BCE onwards (David-Elbiali, 2000; Hafner, 1995). The beginning and
 438 end of the time series are relatively clearly determined. The end results from the *a priori* setting of the
 439 parameter, but also here, as at the beginning of the series, the proxies are very uniform, which explains the
 440 low variability. Overall, the variability is relatively uniform over the entire course of the estimation and
 441 averages over all time slices at 33% of the respective mean.

442 Within the model, the parameter p was estimated, which reflects the relative weight given to the individual
 443 proxies used in the estimation of the number of settlements. This parameter is variable, but has only a
 444 scaling influence on the final estimate of population density.

445 By looking at the distribution of posterior samples for the share of each proxy (Figure 11), it is clear that
 446 the model weights the openness indicator the highest. The average is slightly above 60%. The next most
 447 important indicator is the sum calibration value, which has an average of about 20%. The aoristic sum is
 448 slightly above 10%, whereas the importance of the dendro-dated settlements is below 10%. The reason for the
 449 latter is certainly that there are no lakeshore settlements over large areas of the time window, and therefore
 450 the proxy achieves a low confidence value in comparison with the other estimators. In the case of the aoristic

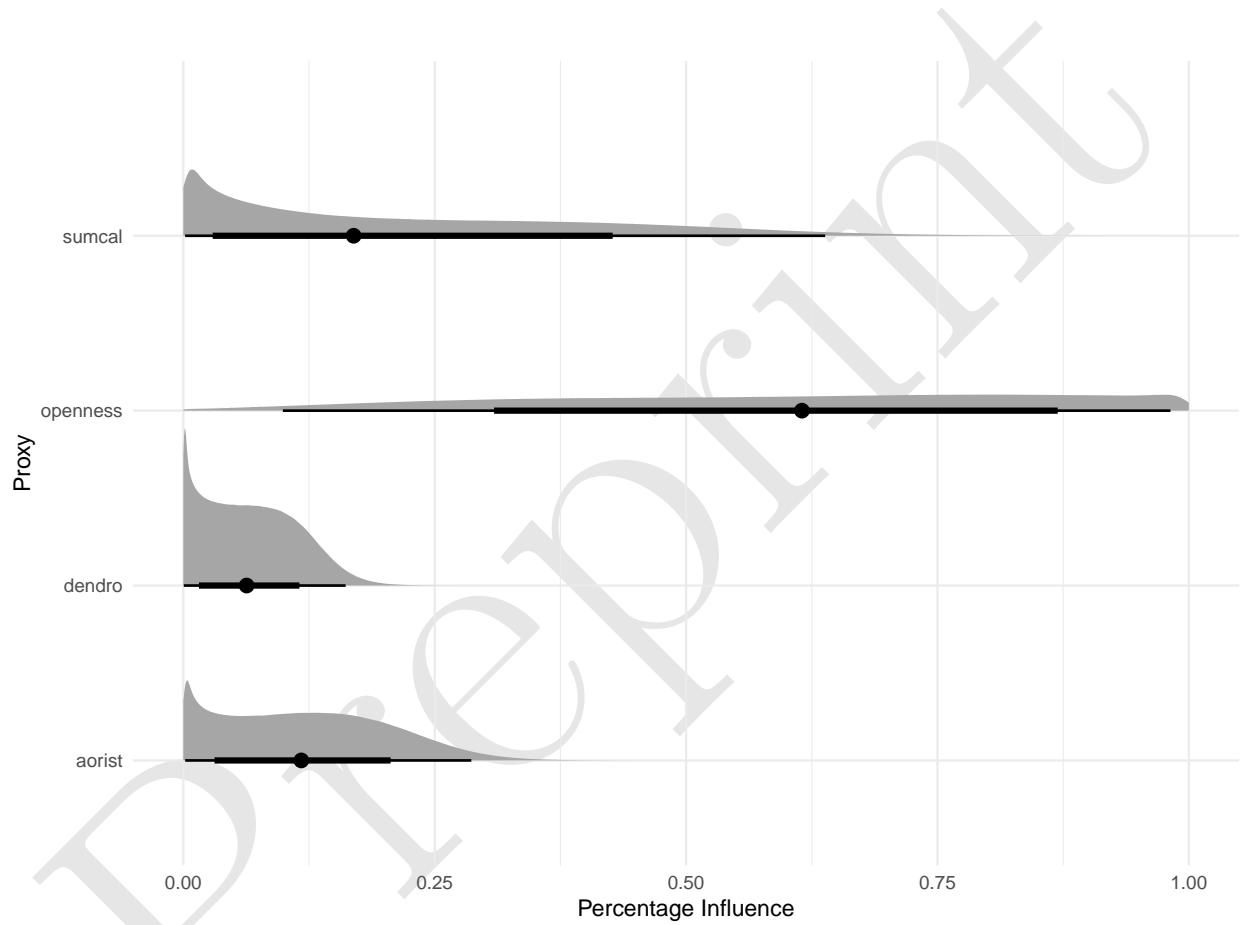


Figure 11: Distribution of the influence ratio of the different proxies on the final estimation of the number of sites.

451 sum, it is certainly the fact that it is flat over large sections and has little structure, making it difficult to
452 relate to the other estimators. The sum calibration shows very strong short-term fluctuations, which are
453 presumably at least partly due to the effects of the calibration curve, and which also make this proxy seem
454 ill-suited to reliably represent a continuous population trend. Nevertheless, its fluctuations do have an impact
455 on the resulting overall estimate of the development of the number of settlements, albeit to a lesser extent.

456 6. Discussion

457 Our original ambition in the development of this model was to base it on a state-space representation of the
458 demographic process itself, and then to integrate the existing proxies by means of an observation model to
459 inform this process. In the course of developing the model, we realised that the data we had available for
460 the case study area north of the Swiss Alps alone was not sufficient to adequately determine this process, or
461 to adequately fix the degrees of freedom resulting from the process and the transfer model. Therefore, in
462 implementation presented here, we have turned to a Poisson regression approach: the model represents the
463 best possible combination of the indicators used to describe the development of the number of sites based on
464 them.

465 6.1. Comparison of individual proxies

466 Comparing the model's overall estimate with trends indicated by individual proxies gives us new insights
467 into the quality of these records. Sum calibration, currently the most frequently used proxy for (relative)
468 population changes in prehistory, has its large fluctuations dampened when considered alongside other proxies.
469 This is especially true for the first fluctuation, shortly after 4000 BCE. The expected increase in archaeological
470 remains with the onset of Neolithisation is still clearly visible, but the curve of the overall estimate, after
471 the initial increase, is much flatter than sum calibration alone indicates. The period between 3950 and 3700
472 BCE, which is contemporaneous with the first larger settlement cycle on the lakeshores of the Three Lakes
473 region, coincides with a noticeable plateau on the calibration curve, which be producing an overestimation of
474 the ^{14}C density. However, the effect of the calibration curve on the results of a cumulative calibration cannot
475 yet be considered unambiguous. A second maximum, after 3000 BCE, is supported by the other proxies, and
476 is consequently also much more clearly reflected in our overall estimate. Here, too plateau in the calibration
477 curve — albeit a smaller, shorter one which is much less pronounced than, for example, the one shortly
478 before between 3350 and 3100. The rise towards the Middle and Late Bronze Age is also supported by the
479 other proxies, especially the aoristic sum, and therefore is preserved in the overall estimate. In this period,
480 the calibration curve does not show any very clear, significant patterns. We may conclude that the model
481 is successful in using information from other proxies to sift 'real' fluctuations in the summed radiocarbon
482 record from artefacts of the calibration curve.

483 On average, the model weights the sum calibration at about 20%, significantly less than the 60% afforded
484 to the openness indicator. After an initial increase, which is easily explained by spread of agriculture,
485 the openness indicator tends to fluctuate less and thus has a dampening effect on the overall estimate.
486 Nevertheless, it appears the general trends in the sum calibration are well reflected in land openness – even if
487 such 'eyeballing' should be interpreted with caution. In contrast to this dramatic trend, changes within the
488 Neolithic and Bronze Age are more gradual, suggestive of larger scale transformations of the landscape. The
489 model is designed rather conservatively by the limit of maximum growth, which is estimated within the model
490 but influences it by its very presence. Therefore, this proxy corresponds better and more homogeneously to a
491 smooth increase in the number of settlements than do the strong fluctuations in the ^{14}C data set.

492 The aoristic sum remains relatively even over long spans of time. It is not until the Middle and Late Bronze
493 Age that we see a significant rise, which is also apparent in the model's overall estimate. It remains to be
494 seen to what extent modelling of the taphonomic loss (Surovell et al., 2009) could be integrated in this
495 approach. We have refrained from doing so in this first model, as this would have introduced further degrees
496 of freedom - but we are aware that with a broader database this would be an interesting possibility, and that
497 it would itself be a variable to be estimated, e.g. in connection with proxies that are not influenced by it
498 (openness indicators, but also data from the demography of burial collectives). This would make it possible

499 to estimate a value from original archaeological material independently of variables that have little to do
500 with archaeological data, such as volcanic eruptions (Ballenger and Mabry, 2011).

501 The number of simultaneously existing lakeshore settlements is a very limited temporal and spatial estimator,
502 but extremely reliable. Its limitations are reflected in the low overall confidence of the model, since its value
503 is zero over long stretches, while other indicators suggest clearly different patterns. However, where it has
504 information potential, such as around and shortly after 3800 BCE, 3200 BCE or especially around 2750 BCE,
505 its fluctuations have a noticeable influence on the overall estimate. The peak around 1600 BCE also leaves a
506 noticeable impact. This highlights another potential of our approach: where a proxy has little structure and
507 thus little significance, or where its trends cannot be linked to other indicators, it consequently has little
508 influence. For periods in which it can provide information, however, this will also feed into the overall model,
509 despite a low overall confidence in the estimator.

510 6.2. Prehistoric population dynamics north of the Swiss Alps

511 In order to review the reconstruction against the background of established archaeological knowledge, it is
512 useful to overlay conventionally-defined archaeological phase boundaries (Hafner, 2005) on the results of our
513 model (Figure 12). It should be noted, however, that the model's estimate is not completely independent of
514 these phases: due to the aoristic sum, which is itself strongly determined by this phase division, corresponding
515 boundaries also influence the structure of the reconstruction. Nevertheless, it helps to check whether the
516 estimate is in strong contradiction to the generally accepted picture or whether it is able to make a credible
517 prediction within this context.

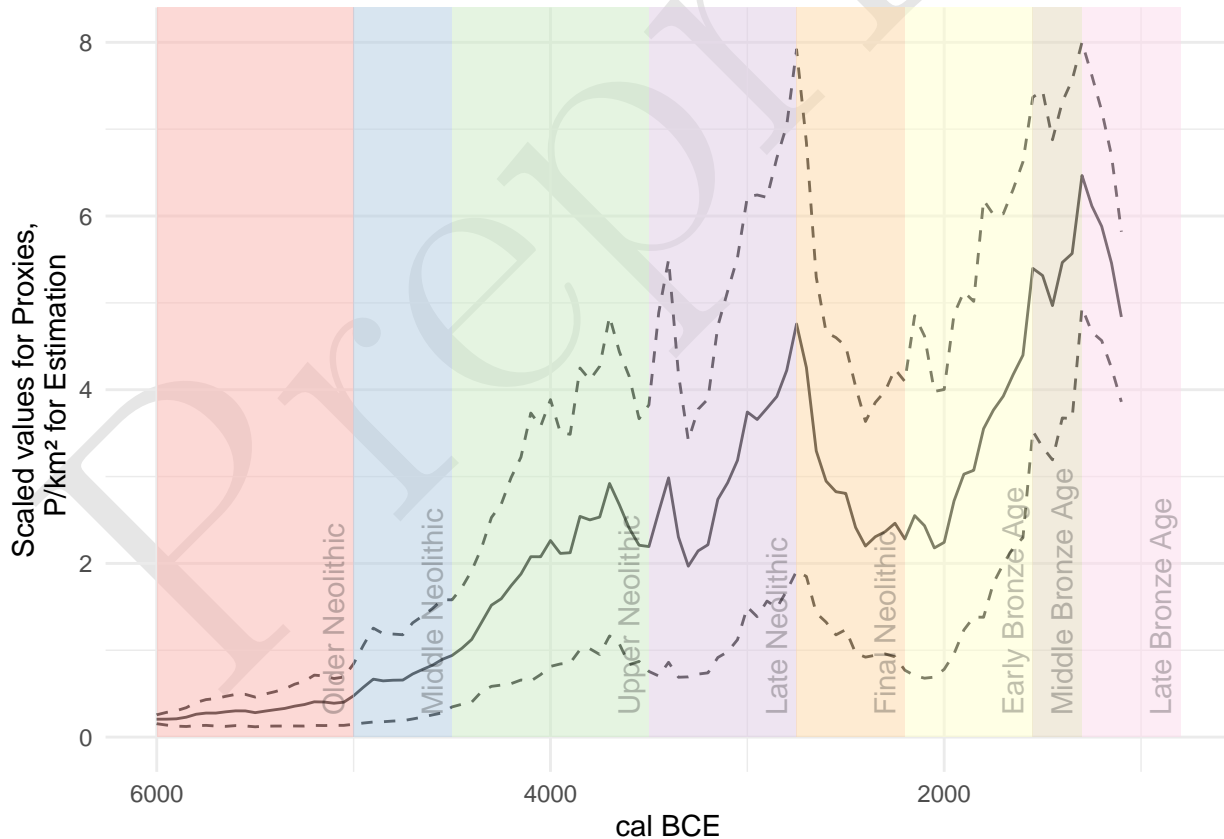


Figure 12: The estimate of the population density in relation to the chronology for the case study area north of the Swiss Alps.

518 The Older and Middle Neolithic phases are in fact hardly documented with known sites in Switzerland. Here
519 we must assume a basically low level of settlement, probably mainly by hunter-gatherer groups. Isolated

520 Neolithic sites of the LBK and later groups are known in the periphery of Switzerland, but they play a
521 subordinate role (Ebersbach et al., 2012). The evidence of the Neolithic especially what the Swiss Plateau is
522 concerned is dense from the so-called Upper Neolithic onwards, connected with the typo-chronological units
523 based on pottery that are called Egolzwil (late 5th M BCE) and Cortaillod respectively Pfyn (first half of the
524 4th M BCE). The first lake shore settlements north of the Alps date to this time too. In this period, we
525 also see a clear increase in the estimated population in the model. In the transition to the Late Neolithic we
526 know from the lakeshore settlements the so-called Horgen Gap (Hafner, 2005). This is also visible as a slight
527 decrease in the model. In another study (Heitz et al., 2021) we could show that this is in fact probably not a
528 decline in population. Rather communities relocated their settlements to the hinterland of the large lakes in
529 times of lake level rises of higher magnitudes due to climatic changes. In the Late Neolithic, associated with
530 the Horgen pottery, we then see a clear increase in the intensity of settlement, which reaches its peak and
531 its break-off at the transition to the Corded Ware and thus to the Final Neolithic (Hafner, 2004). In the
532 second half of the Early Bronze Age, during which – after a break from the Final Neolithic to the very early
533 Bronze Age – lakeshores were resettled, but to a smaller extend. There is again a clear increase in population
534 size according to the model, which continues until the Late Bronze Age. The general trends fit very well
535 with the previous reconstructions of population development for Switzerland (see eg. Lechterbeck et al.,
536 2014). All in all, the estimate of the model corresponds to our expectations, although we must be aware that
537 these expectations are not ‘ground truth’. Nevertheless, we can claim that the model predictions are credible
538 because they accord well with existing knowledge, while offering higher precision and higher resolution.

539 7. Conclusions

540 The key advance in the model we present here is the ability to estimate, in absolute terms, past population
541 sizes and the uncertainty accompanying our present knowledge. These estimates can be used as a basis for
542 further studies where relative measures of population development are not helpful, such as long-term land
543 use studies, where modelling of large-scale socio-ecological systems based on archaeological data becomes
544 possible and does have to rely on using deductive, asynchronous population models (e.g. carrying capacity or
545 ethnographic analogues).

546 We have also demonstrated that, with Bayesian hierarchical modelling, it is possible to achieve a true multi-
547 proxy analysis of prehistoric demographic processes – as opposed to a juxtaposition of different indicators.
548 This opens up the possibility of quantitatively linking different records and assessing their credibility. In
549 addition, and in contrast to existing approaches, we are able to specifying a confidence interval for the overall
550 estimate. The result is a firmer basis for reconstructing population dynamics and settlement patterns in
551 prehistory.

552 Nevertheless, we consider the model present here as only the first step towards a more sophisticated Bayesian
553 approach. We have trusted the individual proxies in aggregate, without considering measurement error.
554 Moreover, our estimates are based on a limited number of sources of evidence, almost all of which are subject
555 to taphonomic biases in the archaeological record (except for the openness indicator). Consequently, we
556 can only transform the model’s prediction into an absolute estimate of population density with predefined
557 parameters: the upper limit of population growth, settlement size and the initial value of the reconstruction.
558 Overcoming this limitation would represent a major refinement of our approach.

559 Incorporating additional proxies that are independent of the immediate, time-dependent conditions of the
560 archaeological record could be one way to achieve this. These could be data on settlement sizes, parameters
561 for economic-ecological carrying capacity, demographic data from burial groups, archaeogenetic data on
562 population sizes, or other records as yet unidentified. This data is available to varying degrees in different
563 regions. On the Swiss Plateau, for example, we have too little data on human remains over large spans of
564 prehistory compared to the abundance of wetland settlements to be able to integrate them meaningful into a
565 model.

566 To apply the model to different regions, the proxies we use here (e.g. the palynological openness indicator)
567 would have to be adapted to fit local conditions and research histories. By means of large-scale modelling,
568 however, it would be possible to supplement gaps in the data in one region with data from other regions by

569 means of regionalisation and a partial transfer of information (partial pooling). Such an extension would
570 be the next logical step in the improvement of the model, to which end we hope to be able to contribute a
571 further study in the near future.

572 **8. Acknowledgements**

573 Large parts of the data collection were conducted as part of the project ‘Beyond lake settlements’ in the
574 doctoral thesis of Julian Laabs, funded by the SNF (project number 152862, PI Albert Hafner). Further
575 data collection was done as part of the XRONOS project, also funded by the SNSF (project number 198153,
576 PI Martin Hinz). The development of the openness index took place within the framework of the project
577 Time and Temporality in Archaeology (project number 194326, PI Caroline Heitz) and was inspired by the
578 cooperation within the project QuantHum (project 169371, PI Marco Conedera), both also funded by the
579 SNSF. Jan Kolář was supported by a long-term research development project (RV67985939) and by a grant
580 from the Czech Science Foundation (19-20970Y). We also thank the Institute of Archaeological Sciences of
581 the University of Bern for its support and faith in the outcome of our modelling project. Finally, we thank
582 (already) the unknown reviewers for their helpful comments, which will certainly improve this manuscript
583 significantly.

584 9. References

- 585 Attenbrow, V., Hiscock, P., 2015. Dates and demography: Are radiometric dates a robust proxy for long-term
586 prehistoric demographic change? *Archaeology in Oceania* 50, 30–36. <https://doi.org/10.1002/arco.5052>
- 587 Ballenger, J.A.M., Mabry, J.B., 2011. Temporal frequency distributions of alluvium in the American
588 Southwest: Taphonomic, paleohydraulic, and demographic implications. *Journal of Archaeological Science*
589 38, 1314–1325. <https://doi.org/10.1016/j.jas.2011.01.007>
- 590 Bryant, J., Zhang, J.L., 2018. Bayesian Demographic Estimation and Forecasting. Chapman; Hall/CRC.
591 <https://doi.org/10.1201/9780429452987>
- 592 Carleton, W.C., Groucutt, H.S., 2021. Sum things are not what they seem: Problems with point-wise
593 interpretations and quantitative analyses of proxies based on aggregated radiocarbon dates. *The Holocene*
594 31, 630–643. <https://doi.org/10.1177/0959683620981700>
- 595 Childe, V.G. (Ed.), 1936. *Man Makes Himself*. Watts & Co., London.
- 596 Christian Lüthi, 2009. Mittelland (region).
- 597 Colton, H.S., 1949. The prehistoric population of the Flagstaff area. *Plateau* 22, 21–25.
- 598 Cook, S.F., 1946. A reconsideration of shell mounds with respect to population and nutrition. *American
599 Antiquity* 12, 51–53.
- 600 Cook, S.F., Heizer, R.F., 1968. Relationships among houses, settlement areas, and population in aboriginal
601 California. *Settlement archaeology* 79–116.
- 602 Cook, S.F., Heizer, R.F., 1965. The Quantitative approach to the relation between population and settlement
603 size. University of California, Archaeological research facility Department of Anthropology, Berkeley,
604 Etats-Unis d'Amérique.
- 605 Crema, E.R., 2022. Statistical Inference of Prehistoric Demography from Frequency Distributions of
606 Radiocarbon Dates: A Review and a Guide for the Perplexed. *Journal of Archaeological Method and
607 Theory*. <https://doi.org/10.1007/s10816-022-09559-5>
- 608 Crema, E.R., Bevan, A., 2021. Inference from large sets of radiocarbon dates: software and methods.
609 *Radiocarbon* 63, 23–39. <https://doi.org/10.1017/RDC.2020.95>
- 610 Crema, E.R., Shoda, S., 2021. A Bayesian approach for fitting and comparing demographic growth models
611 of radiocarbon dates: A case study on the Jomon-Yayoi transition in Kyushu (Japan). *PloS One* 16,
612 e0251695. <https://doi.org/10.1371/journal.pone.0251695>
- 613 David-Elbiali, M., 2000. La Suisse occidentale au IIe millénaire av. J.-C. : Chronologie, culture, intégration
614 européenne. *Cahiers d'archéologie romande*, Lausanne.
- 615 Ebersbach, R., Kühn, M., Stopp, B., Schibler, J., 2012. Die Nutzung neuer Lebensräume in der Schweiz
616 und angrenzenden Gebieten im 5. Jtsd. V. Chr. : Siedlungs- und wirtschaftsarchäologische Aspekte.
617 *Jahrbuch Archäologie Schweiz* 95, 7–34. <https://doi.org/10.5169/SEALS-392483>
- 618 Frankfort, H., 1950. Town planning in ancient Mesopotamia. *Town Planning Review* 21, 98–115.
- 619 French, J.C., Riris, P., Fernández-López de Pablo, J., Lozano, S., Silva, F., 2021. A manifesto for palaeodemography
620 in the twenty-first century. *Philosophical Transactions of the Royal Society B: Biological
621 Sciences* 376, 20190707. <https://doi.org/10.1098/rstb.2019.0707>
- 622 Hack, J.F., 1942. The changing physical environment of the Hopi Indians of Arizona, Papers of the Peabody
623 Mu- seum of American Archaeology and Ethnolog. Harvard University, Cambridge.
- 624 Hafner, A., 2005. Neolithikum: Raum/Zeit-Ordnung und neue Denkmodelle. *Archäologie im Kanton Bern*
625 6B, 431–498.
- 626 Hafner, A., 2004. Vom Spät- zum Endneolithikum. Wandel und Kontinuität um 2700 v. Chr. In *Mitteleuropa.*
627 - Vom Endneolithikum zur Frühbronzezeit: Wandel und Kontinuität zwischen 2400 und 1500 v.Chr, in:
628 Beier, H.J., Einicke, R. (Eds.), *Varia Neolithica. 3. Beiträge Zur Ur- Und Frühgeschichte Mitteleuropas.*
629 Beier&Beran, Weissbach, pp. 213–249.
- 630 Hafner, A., 1995. Die Frühe Bronzezeit in der Westschweiz. Funde und Befunde aus Siedlungen, Gräbern
631 und Horten der entwickelten Frühbronzezeit. *Staatlicher Lehrmittelverlag Bern* 1995, Bern.
- 632 Hassan, F.A., 1981. Demographic archaeology, Studies in archaeology. Academic Press, New York.
- 633 Heitz, C., Hinz, M., Laabs, J., Hafner, A., 2021. Mobility as resilience capacity in northern Alpine Neolithic
634 settlement communities. <https://doi.org/10.17863/CAM.79042>
- 635 Kintigh, K.W., Altschul, J.H., Beaudry, M.C., Drennan, R.D., Kinzig, A.P., Kohler, T.A., Limp, W.F.,
636 Maschner, H.D.G., Michener, W.K., Pauketat, T.R., Peregrine, P., Sabloff, J.A., Wilkinson, T.J., Wright,

- 637 H.T., Zeder, M.A., 2014. Grand challenges for archaeology. *Proceedings of the National Academy of*
 638 *Sciences* 111, 879–880. <https://doi.org/10.1073/pnas.1324000111>
- 639 Kruschke, J.K., 2015. Doing Bayesian Data Analysis. Elsevier. <https://doi.org/10.1016/B978-0-12-405888->
 640 [0.09999-2](#)
- 641 Laabs, J., 2019. Populations- und landnutzungsmodellierung der neolithischen und bronzezeitlichen
 642 westschweiz (PhD thesis). Bern.
- 643 Lechterbeck, J., Edinborough, K., Kerig, T., Fyfe, R., Roberts, N., Shennan, S., 2014. Is Neolithic land
 644 use correlated with demography? An evaluation of pollen-derived land cover and radiocarbon-inferred
 645 demographic change from Central Europe. *The Holocene* 24, 1297–1307. <https://doi.org/10.1177/095968>
 646 [3614540952](#)
- 647 Martínez-Grau, H., Morell-Rovira, B., Antolín, F., 2021. Radiocarbon Dates Associated to Neolithic Contexts
 648 (Ca. 5900 – 2000 Cal BC) from the Northwestern Mediterranean Arch to the High Rhine Area. *Journal*
 649 *of Open Archaeology Data* 9, 1. <https://doi.org/10.5334/joad.72>
- 650 Morris, I., 2013. The measure of civilization: How social development decides the fate of nations. Princeton
 651 University Press, Princeton.
- 652 Müller, J., Diachenko, A., 2019. Tracing long-term demographic changes: The issue of spatial scales. *PLOS*
 653 *ONE* 14, e0208739. <https://doi.org/10.1371/journal.pone.0208739>
- 654 Naroll, R., 1962. Floor Area and Settlement Population. *American Antiquity* 27, 587–589. <https://doi.org/>
 655 [10.2307/277689](#)
- 656 Nikulka, F., 2016. Archäologische Demographie. Methoden, Daten und Bevölkerung der europäischen Bronze-
 657 und Eisenzeiten. Sidestone Press, Leiden.
- 658 Ramsey, C.B., 1995. Radiocarbon calibration and analysis of stratigraphy; the OxCal program. *Radiocarbon*
 659 37, 425430.
- 660 Rick, J.W., 1987. Dates as Data: An Examination of the Peruvian Preceramic Radiocarbon Record. *American*
 661 *Antiquity* 52, 55–73. <https://doi.org/10.2307/281060>
- 662 Riede, F., 2009. Climate and demography in early prehistory: Using calibrated (14)C dates as population
 663 proxies. *Human Biology* 81, 309–337. <https://doi.org/10.3378/027.081.0311>
- 664 Schiffer, M.B., 1987. Formation processes of the archaeological record. University of New Mexico Press,
 665 Albuquerque-NM.
- 666 Schmidt, I., Hilpert, J., Kretschmer, I., Peters, R., Broich, M., Schiesberg, S., Vogels, O., Wendt, K.P.,
 667 Zimmermann, A., Maier, A., 2021. Approaching prehistoric demography: Proxies, scales and scope of the
 668 Cologne Protocol in European contexts. *Philosophical Transactions of the Royal Society B: Biological*
 669 *Sciences* 376, 20190714. <https://doi.org/10.1098/rstb.2019.0714>
- 670 Shennan, S., 2000. Population, Culture History, and the Dynamics of Culture Change. *Current Anthropology*
 671 41, 811–835.
- 672 Shennan, S., Downey, S.S., Timpson, A., Edinborough, K., Colledge, S., Kerig, T., Manning, K., Thomas,
 673 M.G., 2013. Regional population collapse followed initial agriculture booms in mid-Holocene Europe.
 674 *Nature Communications* 4, 2486. <https://doi.org/10.1038/ncomms3486>
- 675 Surovell, T.A., Byrd Finley, J., Smith, G.M., Brantingham, P.J., Kelly, R., 2009. Correcting temporal
 676 frequency distributions for taphonomic bias. *Journal of Archaeological Science* 36, 1715–1724. <https://doi.org/10.1016/j.jas.2009.03.029>
- 677 Turchin, P., Brennan, R., Currie, T., Feeney, K., Francois, P., Hoyer, D., Manning, J., Marciniak, A., Mullins,
 678 D., Palmisano, A., Peregrine, P., Turner, E.A.L., Whitehouse, H., 2015. Sesat: The Global History
 679 Databank. *Cliodynamics* 6. <https://doi.org/10.21237/C7clio6127917>
- 680 Zimmermann, A., 2004. Landschaftsarchäologie II. Überlegungen zu prinzipien einer landschaftsarchäologie.

682 10. Author contributions

- 683 • *Martin Hinz*: Conceptualization, Methodology, Software, Validation, Formal analysis, Investigation,
684 Data Curation, Writing - Original Draft, Writing - Review & Editing, Visualization
685 • *Joe Roe*: Software, Validation, Writing - Review & Editing,
686 • *Julian Laabs*: Investigation, Data Curation, Writing - Review & Editing,
687 • *Caroline Heitz*: Conceptualization, Investigation, Writing - Review & Editing,
688 • *Jan Kolář*: Conceptualization, Writing - Review & Editing,

689 11. Colophon

690 This report was generated on 2022-05-30 10:07:15 using the following computational environment and
691 dependencies:

```
692 #> - Session info -----  
693 #>   setting  value  
694 #>   version R version 4.2.0 (2022-04-22)  
695 #>   os        Manjaro Linux  
696 #>   system   x86_64, linux-gnu  
697 #>   ui        X11  
698 #>   language (EN)  
699 #>   collate   C  
700 #>   ctype     de_DE.UTF-8  
701 #>   tz        Europe/Zurich  
702 #>   date      2022-05-30  
703 #>   pandoc    2.17.1.1 @ /usr/bin/ (via rmarkdown)  
704 #>  
705 #> - Packages -----  
706 #>   package * version date (UTC) lib source  
707 #>   assertthat 0.2.1  2019-03-21 [1] CRAN (R 4.2.0)  
708 #>   bitops     1.0-7  2021-04-24 [1] CRAN (R 4.2.0)  
709 #>   bookdown   0.26   2022-04-15 [1] CRAN (R 4.2.0)  
710 #>   brio       1.1.3   2021-11-30 [1] CRAN (R 4.2.0)  
711 #>   cachem     1.0.6   2021-08-19 [1] CRAN (R 4.2.0)  
712 #>   callr       3.7.0   2021-04-20 [1] CRAN (R 4.2.0)  
713 #>   class      7.3-20  2022-01-16 [2] CRAN (R 4.2.0)  
714 #>   classInt   0.4-3   2020-04-07 [1] CRAN (R 4.2.0)  
715 #>   cli         3.3.0   2022-04-25 [1] CRAN (R 4.2.0)  
716 #>   colorspace  2.0-3   2022-02-21 [1] CRAN (R 4.2.0)  
717 #>   cowplot    * 1.1.1   2020-12-30 [1] CRAN (R 4.2.0)  
718 #>   crayon     1.5.1   2022-03-26 [1] CRAN (R 4.2.0)  
719 #>   curl        4.3.2   2021-06-23 [1] CRAN (R 4.2.0)  
720 #>   DBI        1.1.2   2021-12-20 [1] CRAN (R 4.2.0)  
721 #>   desc        1.4.1   2022-03-06 [1] CRAN (R 4.2.0)  
722 #>   devtools    2.4.3   2021-11-30 [1] CRAN (R 4.2.0)  
723 #>   digest      0.6.29  2021-12-01 [1] CRAN (R 4.2.0)  
724 #>   dplyr       1.0.9   2022-04-28 [1] CRAN (R 4.2.0)  
725 #>   e1071      1.7-9   2021-09-16 [1] CRAN (R 4.2.0)  
726 #>   ellipsis    0.3.2   2021-04-29 [1] CRAN (R 4.2.0)  
727 #>   evaluate    0.15    2022-02-18 [1] CRAN (R 4.2.0)  
728 #>   fansi       1.0.3   2022-03-24 [1] CRAN (R 4.2.0)  
729 #>   farver      2.1.0   2021-02-28 [1] CRAN (R 4.2.0)  
730 #>   fastmap    1.1.0   2021-01-25 [1] CRAN (R 4.2.0)  
731 #>   foreign    0.8-82  2022-01-16 [2] CRAN (R 4.2.0)
```

```

732 #> fs           1.5.2   2021-12-08 [1] CRAN (R 4.2.0)
733 #> generics     0.1.2   2022-01-31 [1] CRAN (R 4.2.0)
734 #> ggmap        * 3.0.0   2019-02-05 [1] CRAN (R 4.2.0)
735 #> ggplot2      * 3.3.6   2022-05-03 [1] CRAN (R 4.2.0)
736 #> ggrepel       * 0.9.1   2021-01-15 [1] CRAN (R 4.2.0)
737 #> ggsn         * 0.5.0   2019-02-18 [1] CRAN (R 4.2.0)
738 #> glue          1.6.2   2022-02-24 [1] CRAN (R 4.2.0)
739 #> gtable        0.3.0   2019-03-25 [1] CRAN (R 4.2.0)
740 #> here          * 1.0.1   2020-12-13 [1] CRAN (R 4.2.0)
741 #> highr         0.9     2021-04-16 [1] CRAN (R 4.2.0)
742 #> htmltools     0.5.2   2021-08-25 [1] CRAN (R 4.2.0)
743 #> httr          1.4.3   2022-05-04 [1] CRAN (R 4.2.0)
744 #> jpeg          0.1-9   2021-07-24 [1] CRAN (R 4.2.0)
745 #> KernSmooth    2.23-20  2021-05-03 [2] CRAN (R 4.2.0)
746 #> knitr         1.39    2022-04-26 [1] CRAN (R 4.2.0)
747 #> labeling       0.4.2   2020-10-20 [1] CRAN (R 4.2.0)
748 #> lattice        0.20-45  2021-09-22 [2] CRAN (R 4.2.0)
749 #> lifecycle      1.0.1   2021-09-24 [1] CRAN (R 4.2.0)
750 #> magrittr       2.0.3   2022-03-30 [1] CRAN (R 4.2.0)
751 #> maptools       1.1-4   2022-04-17 [1] CRAN (R 4.2.0)
752 #> memoise        2.0.1   2021-11-26 [1] CRAN (R 4.2.0)
753 #> munsell        0.5.0   2018-06-12 [1] CRAN (R 4.2.0)
754 #> pillar         1.7.0   2022-02-01 [1] CRAN (R 4.2.0)
755 #> pkgbuild       1.3.1   2021-12-20 [1] CRAN (R 4.2.0)
756 #> pkgconfig      2.0.3   2019-09-22 [1] CRAN (R 4.2.0)
757 #> pkgload         1.2.4   2021-11-30 [1] CRAN (R 4.2.0)
758 #> plyr           1.8.7   2022-03-24 [1] CRAN (R 4.2.0)
759 #> png             0.1-7   2013-12-03 [1] CRAN (R 4.2.0)
760 #> prettyunits    1.1.1   2020-01-24 [1] CRAN (R 4.2.0)
761 #> processx       3.5.3   2022-03-25 [1] CRAN (R 4.2.0)
762 #> proxy          0.4-26  2021-06-07 [1] CRAN (R 4.2.0)
763 #> ps              1.7.0   2022-04-23 [1] CRAN (R 4.2.0)
764 #> purrr          0.3.4   2020-04-17 [1] CRAN (R 4.2.0)
765 #> R6              2.5.1   2021-08-19 [1] CRAN (R 4.2.0)
766 #> RColorBrewer   1.1-3   2022-04-03 [1] CRAN (R 4.2.0)
767 #> Rcpp            1.0.8.3  2022-03-17 [1] CRAN (R 4.2.0)
768 #> remotes         2.4.2   2021-11-30 [1] CRAN (R 4.2.0)
769 #> rgdal           1.5-32  2022-05-09 [1] CRAN (R 4.2.0)
770 #> RgoogleMaps    1.4.5.3  2020-02-12 [1] CRAN (R 4.2.0)
771 #> rjson            0.2.21  2022-01-09 [1] CRAN (R 4.2.0)
772 #> rlang            1.0.2   2022-03-04 [1] CRAN (R 4.2.0)
773 #> rmarkdown        2.14    2022-04-25 [1] CRAN (R 4.2.0)
774 #> rnaturalearth   * 0.1.0   2017-03-21 [1] CRAN (R 4.2.0)
775 #> rprojroot        2.0.3   2022-04-02 [1] CRAN (R 4.2.0)
776 #> rstudioapi       0.13    2020-11-12 [1] CRAN (R 4.2.0)
777 #> s2              1.0.7   2021-09-28 [1] CRAN (R 4.2.0)
778 #> scales           1.2.0   2022-04-13 [1] CRAN (R 4.2.0)
779 #> sessioninfo     1.2.2   2021-12-06 [1] CRAN (R 4.2.0)
780 #> sf               * 1.0-7   2022-03-07 [1] CRAN (R 4.2.0)
781 #> sp               * 1.4-7   2022-04-20 [1] CRAN (R 4.2.0)
782 #> stringi          1.7.6   2021-11-29 [1] CRAN (R 4.2.0)
783 #> stringr          1.4.0   2019-02-10 [1] CRAN (R 4.2.0)
784 #> testthat         3.1.4   2022-04-26 [1] CRAN (R 4.2.0)
785 #> tibble           3.1.7   2022-05-03 [1] CRAN (R 4.2.0)

```

```
786 #> tidyverse      1.2.0  2022-02-01 [1] CRAN (R 4.2.0)
787 #> tidyselect      1.1.2  2022-02-21 [1] CRAN (R 4.2.0)
788 #> units          0.8-0  2022-02-05 [1] CRAN (R 4.2.0)
789 #> usethis        2.1.5  2021-12-09 [1] CRAN (R 4.2.0)
790 #> utf8           1.2.2  2021-07-24 [1] CRAN (R 4.2.0)
791 #> vctrs           0.4.1  2022-04-13 [1] CRAN (R 4.2.0)
792 #> withr          2.5.0  2022-03-03 [1] CRAN (R 4.2.0)
793 #> wk              0.6.0  2022-01-03 [1] CRAN (R 4.2.0)
794 #> xfun            0.31   2022-05-10 [1] CRAN (R 4.2.0)
795 #> yaml            2.3.5  2022-02-21 [1] CRAN (R 4.2.0)
796 #>
797 #> [1] /home/martin/R/x86_64-pc-linux-gnu-library/4.2
798 #> [2] /usr/lib/R/library
799 #>
800 #> -----
```